UNIVERSITÀ DEGLI STUDI DI TRIESTE

XXXIV CICLO DEL DOTTORATO DI RICERCA IN

BIOMEDICINA MOLECOLARE

ITGA6 is a key molecule in driving metastatization of platinum resistant epithelial ovarian cancer

Settore scientifico-disciplinare: BIO/11 BIOLOGIA MOLECOLARE

ANNO ACCADEMICO 2020/2021

This PhD project was carried out at Centro di Riferimento Oncologico (CRO, National Cancer Institute) of Aviano, in the Division of Molecular Oncology directed by Dr. Gustavo Baldassarre

A Enrica, una promessa.

“Accompagnarla fino all’ultimo è stato un privilegio come lo è stato vivere con lei questi ultimi vent’anni.

Le ho chiesto: hai qualcosa che mi vuoi dire? Mi ha risposto: Non dimenticatemi!”

8 Novembre 2016

Table of contents

ABSTRACT

Epithelial ovarian cancer (EOC) is a relatively rare disease usually diagnosed in advanced stages (III and IV stage). Standard of care includes radical surgery followed by platinum-based chemotherapy. Yet, 15% to 30% of EOC patients have a primary platinum-resistant or refractory disease and more than 70% of originally platinum-sensitive advanced stages patients will develop a resistant disease disseminated in the abdomen and pelvis. For these reasons, the net five-year survival by stage is only of 26% and 13% for stage III and IV, respectively. The resistance to chemotherapy is one of the major challenges cancer research faces nowadays. In our lab, we have established several Platinum (PT) resistant (PT-res) cellular models to better understand the molecular pathways that could guide PT-resistance in ovarian cancer. We observed that one of the common features of these PT-res cells was the higher ability to adhere on the mesothelial cells respect to their sensitive counterpart, a fundamental capacity for driving cell dissemination into the peritoneal cavity.

My PhD project focused the attention on the dissection of the molecular basis of the higher adhesion capability of PT-res cells to possibly identify new therapeutic targets to overcome EOC peritoneal dissemination. We found all tested PT-res cells over-expressed the integrin alpha 6 (ITGA6) protein that in turn mediated their higher ability to adhere and migrate on the specific substrate laminin (LM) and on mesothelial cells. Using pharmacological and genetic tools, we showed that ITGA6 expression was linked to a higher capacity of PT-res cells to form ovaryspheres *in vitro* and to grow and disseminate *in vivo*. Molecular analyses next demonstrated that under PT treatment positively regulated ITGA6 gene promoter activity by via the SP1 transcription factor, possibly explaining the higher ITGA6 expression in PT-res cells. Moreover, PT-treatment also induced an active secretion of ITGA6. Once secreted, ITGA6 on one side primed mesothelial cells to form a pro-metastatic niche and, on the other, favoured the spreading of neighbour tumour cells. Mechanistically, the engagement of ITGA6 with LM positively regulated Snail expression favouring cell adhesion and spreading. These in vitro data were recapitulated in the human pathology since we found higher ITGA6 levels in the ascitic fluids of EOC patients with a PT-resistant disease and also demonstrated that higher levels of circulating ITGA6 could be found in the plasma of EOC after PT-based chemotherapy. Altogether, our collected data suggested that ITGA6 could be a reasonable druggable target to prevent EOC metastatization and dissemination in the peritoneal cavity, for instance by the use of specific blocking antibodies. Moreover, since ITGA6 is easily quantifiable in the circulation of EOC patients it could be used as predictive biomarkers to identify patients that could not respond to the standard PT-based chemotherapy

1.INTRODUCTION

1.1 Epithelial Ovarian cancer: classification and metastatic colonization.

Ovarian cancer is the most aggressive of gynecological cancers, affecting about 240,000 women every year worldwide [1] and despite the low incidence rate, it represents the eighth cause of cancer-dependent death among women. The prognosis of this disease is thus poor due to three main factors: the high molecular and pathological heterogeneity, the late diagnosis and the high incidence of therapy-resistant relapses.

Histologically, ovarian cancer refers to a heterogeneous group of diseases originating from three different cell types: germinal, stromal and epithelial.

The most representative group among these types of tumours is the epithelial ovarian cancer (EOC) (90%). It originates from the epithelium surrounding the ovaries (OSE) and can be divided into four different histological subtypes: **serous** (52% of cases), **mucinous** (6%), **endometrioid** (10%), and "**clear cells**" (6%) which reflects the characteristics of the fallopian tubes, endocervix and endometrium [2].

Based on molecular and genetic characteristics, EOCs can be divided into type I and type II tumors[3].

- **Type I (25%)** includes mucinous, clear cell, low grade serous and low grade endometrioid carcinoma. They are generally well-differentiated, slow-growing tumours usually diagnosed in the early stages of the disease and characterized by BRAF, KRAS, β-catenin and PTEN mutations[1].
- **Type II (75%)** includes high-grade serous and high-grade endometrioid types. They are more aggressive since they growth and disseminate with higher frequency. They show a genomic instability with abnormal number of DNA copies and mutations affecting p53, BRCA1 / 2, NF1 and RB1 genes.

Finally, ovarian cancer can be classified according to its degree of differentiation (according to the International Federation of Gynecology and Obstetrics, FIGO) into four stages (I, II, III and IV stage), with a different rate of 5-year **survival** from diagnosis [1 4].

- I stage: the tumour mass is confined to the ovaries and fallopian tubes, the 5-year survival is 89%;
- II stage: the neoplastic cells have already reached the pelvic cavity and 65% of patients survive up to 5 years;
- III stage: presence of metastases in the peritoneal region and lymph node areas; 5-year survival is 22%;
- IV stage: metastases present beyond the peritoneal region; in this case the 5-year survival drops drastically to 13%.

As stated, despite its low incidence, in about 70% of cases the diagnosis of the disease occurs when the tumour has already reached an advanced stage; this is due to the lack of screening procedures and

to the absence of symptoms in the initial stages. The disease, in fact, develops in the peritoneal cavity causing abdominal swelling and other symptoms that can be easily confused and erroneously attributed to other pathologies[5] [6]. Moreover, late diagnosis of ovarian cancer leads to metastases formation facilitating also by the lack of anatomical barriers that limit the spread of cancer cells from the ovary to the peritoneal cavity. From the tumour primary site, metastasis process starts, since the cell-cells contact are missing[7] and the neoplastic cells undergo passive dissemination assisted by the flow of peritoneal fluid[8]. In this context, tumour epithelial cells, floating in the peritoneal fluid as aggregates or spheroids, are able to overcome cell death and escape immunosurveillance[9]. During the disease progression there is an increase of ascites production and it is possible to observe the invasion of the abdomen by cancer cells that reach the omentum[10], which is the predominant site of ovarian cancer metastasis (Figure 1). In this setting all the organs within the peritoneal cavity are lined with a single layer of mesothelial cells that cover an underlying stroma composed of an extracellular matrix (ECM) and stromal cells (STC). The floating ovarian cancer cells attach to this layer, invade through the mesothelial cell barrier into the peritoneum, omentum, and bowel serosa. The ECM is composed by elastin, fibrillin, fibulins, fibrinogen, fibronectin, laminin, tenascins and thrombospondins, while STC cells are composed by fibroblast (CAFs), endothelial cells , adipocytes and immune cells[9] ECM and STC are some of the element sustaining tumoural microenvironment that is thus involved in each step of peritoneal dissemination. Furthermore, several studies have shown that tumour cells are able to modify the microenvironment also by releasing cancer cell-derived exosomes that reprogram or educate other cells to support tumour survival and promote metastasis. It is also well known that the exosomes mediate crosstalk between cancer cells and microenvironment and represent useful diagnostic and prognostic biomarkers[11].

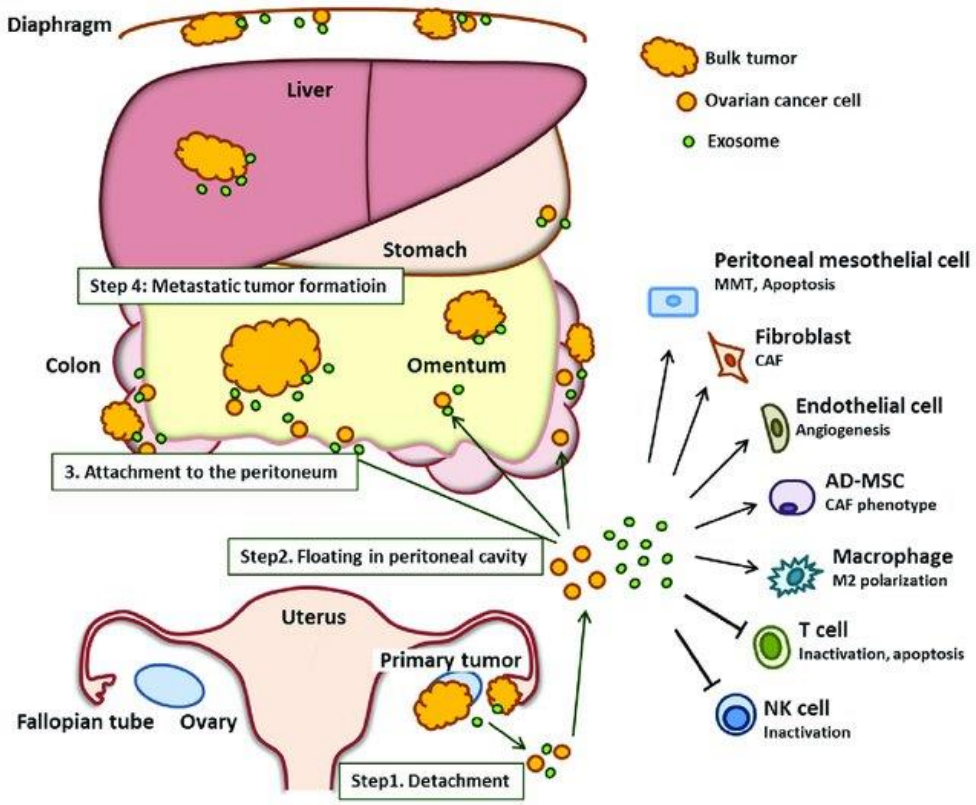

Figure 1: Overview of ovarian cancer dissemination in the peritoneal cavity. Four steps are shown. **Step1**. Ovarian cancer cells detachment from the primary tumor and exosome derived secretion. **Step2**. Floating in the peritoneal cavity in spheroids formation.**Step3** Attachment to the peritoneum. **Step4** Metastatic tumor formation[11].

1.1.2 EOC therapies. Despite the classification, all EOC patients are equally treated in first instance with cytoreductive surgery followed by chemotherapy. In patients with tumour confined to the ovary, surgery alone is curative for more than 90%. However, in most cases the tumour has already spread to other organs. The goal of primary surgery, defined as optimal cytoreduction, is the absence of residual cancer. After surgery, adjuvant chemotherapy is mandatory in cases of suboptimal debulking (residual disease of 1 cm or more), advanced stages, or early stages with a high risk of recurrence[12]. The two classes of drugs mostly used in ovarian cancer are **platinum** compounds and **taxanes**. Paclitaxel belongs to the taxanes family drugs that act on microtubles, producing destabilization in cytoskeletal, organelles, vescicles and cells division[13]. Platinum agents (e.g cisplatin and carboplatin) are the most used in clinics for EOC treatment since Lambert and Berry showed better outcomes for cisplatin-cyclophosphamide compared with cyclophosphamide alone[14]. Subsequently, the cisplatin-paclitaxel combination was demonstrated to be more effective than cisplatin-cyclophosphamide[15]. These compounds are used in many types of cancer, able to interfere with all phases of the cell cycle by binding to DNA through the formation of cross-links between complementary strands. Cisplatin, because of its dose-limiting toxicity including minor symptoms like nausea and serious injuries on kidney and peripheral neuropathy, it has been replaced by carboplatin, with comparable efficacy but less toxicity respect to cisplatin. Thus, from the early 2000s, carboplatin in combination with

paclitaxel has been the standard of care in the adjuvant and first-line settings. In addition to Paclitaxel, other agents are used in combination with platinum chemotherapy, especially in the relapse setting, including liposomal pegylated doxorubicin (PLD), gemcitabine, and bevacizumab (Chandra et al., 2019). The combination carboplatin-PLD was explored in the MITO-2 trial, however no differences in the Progression Free Survival (PFS) between the patients were observed even if it represent a less toxic alternative[16]. **Bevacizumab** (Avastin®; Genentech, San Francisco, CA, USA) is a humanized monoclonal antibody that binds to vascular endothelial growth factor A (VEGF-A) and is recognized as a potent antiangiogenic agent. Another class of drugs approved in clinics are the poly(adenosine diphosphate–ribose) polymerase **(PARP) inhibitors** (e.g. Olaparib, Niraparib, Niraparib) that provided a substantial progression-free survival benefit as maintenance monotherapy in BRCA1/2 mutated patients with a complete or partial clinical response after platinum-based chemotherapy[17]. On May 2020, the FDA approved for this class of patients bevacizumab in combination with Olaparib for first-line **maintenance** treatment[18]. Although many advances have been made in the treatment of ovarian cancer, the standard care is still the one with platinum compounds. Therefore, understanding resistance mechanisms to find new target therapies remains a challenge.

1.1.3 Mechanisms of Cisplatin resistance. Although 70-80% of ovarian cancer patients respond well to first-line therapy, most of them relapse within two years, requiring second-line chemotherapy. In this regard, based on the time relapsed between the end of platinum-based treatment and relapse, referred to as platinum-free interval, patients are classified in (Figure 2):

• **refractory**, when cancer progresses during first-line therapy;
• **resistant,** when patients relapse within 6 months of treatment;
• **partially sensitive**, when the relapse occurs 6 months after treatment;
• **sensitive**, when the relapse occurs beyond the following 12 months.

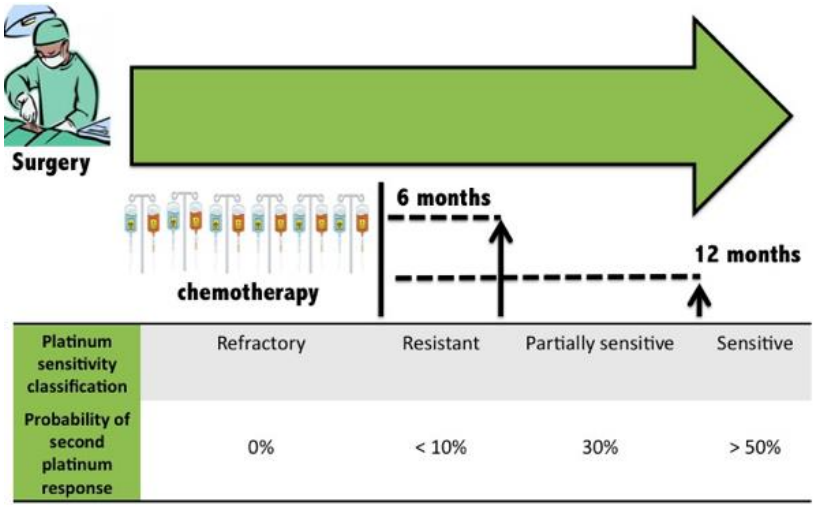

Figure 2: Platinum-resistance definition by the Gynecologic Oncology Group (GOG). Platinum sensitivity is classified as resistant, partially sensitive, or sensitive, according to the time relapsed since finishing first-line treatment. Probability of re-treatment response is shown for each group of patients.

Based on the Cisplatin (hereafter CDDP) effect in the cells there are different mechanisms of resistance. CDDP exerts anticancer effects via an interrelated signalling pathway that might be separated into one nuclear and one cytoplasmic module. CDDP is inert and must be intracellularly activated by a series of aquation reactions that consist in the substitution of one or both cis-chloro groups with water molecules. This exchange of molecule occurs spontaneously in the cytoplasm, generating the highly reactive mono- and bi-aquated CDDP forms. These molecules are prone to interact with a wide number of cytoplasmic substrates, and in particular with endogenous nucleophiles such as reduced glutathione (GSH), methionine, metallothioneins and proteins (via their cysteine residues). Thus, cytoplasmic CDDP has the potential to deplete reduced equivalents and to tilt the redox balance toward **oxidative stress**. On the other hand, in the nucleus, aquated cisplatin avidly binds DNA, with a predilection for nucleophilic N7-sites on **purine** bases. This leads to the generation of protein–DNA complexes as well as of DNA–DNA inter- and intra-strand adducts, producing DNA lesions committing cells to death (Figure 3).

The CDDP resistance mechanisms are classify in four different type[19]:

- ✓ **Mechanisms of pre-target resistance** occurs when cancer cells elude the cytotoxic potential of CDDP before it binds to cytoplasmic targets and DNA. There is a reduced intracellular accumulation of CDDP (due to an increased efflux via relatively nonselective members of the ATP-binding cassette (ABC) family or other transporters[20]) and an increased sequestration of CDDP by GSH, metallothioneins[21] and other cytoplasmic proteins with nucleophilic properties.

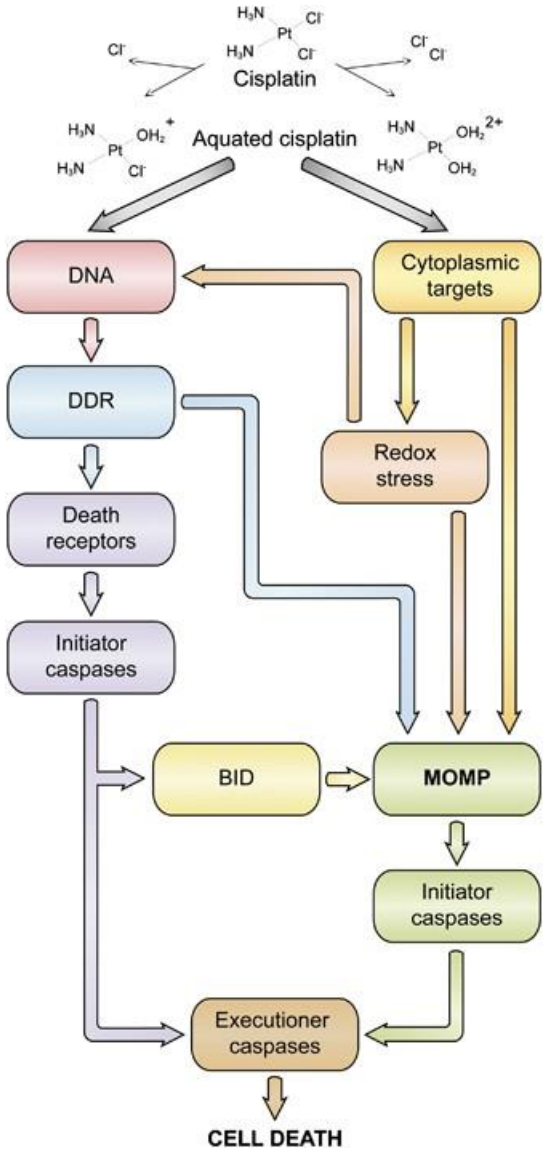

Figure 3: Cisplatin effects in the cells. Cisplatin in the cytoplasmic causes oxidative stress that lead to mitochondrial outer membrane permeabilization (MOMP), thereby triggering intrinsic apoptosis. In the nucleus the cisplatin bind the DNA causing lesion and lead to death the cells[19].

✓ **Mechanisms of on-target resistance** occurs when the majority of CDDP lesions are removed from DNA by the nucleotide excision repair (NER) system. Early reports pointed to a correlation between NER proficiency and CDDP resistance in multiple preclinical models. Thus, ERCC1 expression has been negatively correlated with survival and/or responsiveness to CDDP-based regimens in several human neoplasms, as for other **DNA damage response alteration**[22]**.**

✓ **Mechanisms of post-target resistance.** They can result from a plethora of alterations including defects in signal transduction pathways as apoptosis in response to DNA damage. One of the most predominant mechanisms of post-target resistance involves the **inactivation of TP53**[23], which occurs in approximately half of all human neoplasms. Thus, ovarian cancer patients harboring wild-type TP53 have a higher probability to benefit from CDDP-based chemotherapy than patients with TP53 mutations[24] [25]. Another survival signalling activated could be the induction of **epithelial-mesenchymal transition (EMT)** through the SNAIL and SLUG activation. Thus, CDDP triggers the EMT mechanism: EMT process is involved in the transformation of static epithelial cells into mobile mesenchymal cells and is a crucial event for tumour metastasis and migration[26].

✓ **Mechanisms of off-target resistance**. CDDP-resistant phenotype can also be sustained (if not entirely generated) by alterations in signalling pathways that are not directly engaged by CDDP but influenced by the microenvironment and compensate lethal signals. Some tumour cells (the cancer stem cells CSCs) due to unfavourable microenvironment (such as hypoxia, nutrient stress, and lack of growth factors) may enter dormancy. Non-quiescent tumour cells are eliminated by

chemotherapy and when favourable microenvironment is restored, these dormant cells can repopulate the tumour[27]. CSCs are located in *niche* and specific components of ECM are involved in their sustaining. For this reason ECM may contribute to chemotherapy resistance[28]. In addition, ECM has been shown to modulate tumour dormancy and serve as a "gatekeeper" in transition from quiescence to proliferation of cancer cells[29]. Environmental mediated drug resistance regard also the not dormant cells. The binding to ECM components, (cell adhesion-mediated drug resistance CAM-DR), allows to the cells to escape cytotoxic stress rapidly at a non-genetic basis and lead to subsequent genetic adaptations. The matrix-associated cells persist and repopulate the tumour after chemotherapy, resulting in recurrence. Integrins in particular were found as CAM-DR marker associated with a shorter PFS[30].

1.2 Integrins structure and functions.

Integrins represent the largest known class of transmembrane adhesion receptors and are involved in the mediation of cell-cell and cell-extracellular matrix (ECM) interactions, as well as a variety of cell bonds with various pathogens [31 32]. Integrins are transmembrane glycoproteins composed of 18 α and 8 β subunits [33] that are non-covalently associate to form pairs of heterodimers: each of them is specific for extracellular matrix proteins (ECM) or for ligands present on cell surface. Depending on the αβ association, integrins can generate multiple intracellular responses, since they can associate with different domains of different ligands, which can be the target of multiple integrins. They can be divided into four sub-families [34]: **collagen receptors, laminin receptors,** specific **receptors for leukocytes** and Arginine-Glycine-Aspartic Acid (**RGD) residue receptors**.

The structure of the **α-subunit** consists of a seven-bladed β-propeller domain, which forms the head, a thigh domain, two calf domains, a single transmembrane domain and a short cytoplasmic tail (Figure 4). α-subunits can be grouped according to whether or not they contain an inserted (I) domain ('αI' domain). When present, the αI domain in α-subunits forms the major ligand-binding site and it is inserted between β-sheets 2 and 3 in the β-propeller. The αI domain is necessary for collagen receptors (α1, α2, α10 and α11) and the leukocyte receptors (αE, αL, αM, αD and αX)[35]. The α subunits are similar to Position-Specific (PS) integrin protein in Drosophila. Thus, on the lack for αI they are classified in four subfamilies based on evolutionary lineage.

-**PS1** cluster, sharing the same structure of the drosophila PS1 proteins, are **laminin** receptors (α3, α6 and α7),

-**PS2** cluster, sharing the same structure of the drosophila PS2 proteins are Arg-Gly-Asp (RGD) sequence receptors (αIIb, αv, α5 and α8),

-**PS3** is only found in invertebrates,

-**PS4** is known as the α4/α9 cluster and comprises the α4 and α9 subunits.

The structure of **β-subunit** consists of a head region, a leg section, a transmembrane (TM) domain and a cytoplasmic tail. The head region is composed of a βI domain, which is near the hybrid domain that attaches to the plexin–semaphorin–integrin (PSI) domain. Then the leg section contains four cysteine-rich integrin epidermal growth factor-like (I-EGF) modules, before the TM domain and a cytoplasmic tail (Figure 4).

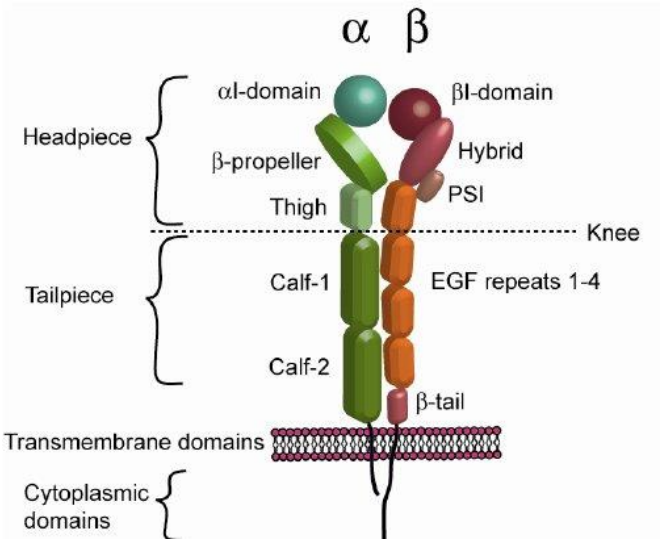

Figure 4: Schematic illustration of the integrin structure. Integrin α (in green) and β (in red) subunits consist of extracellular, transmembrane, and intracellular domains. As described in the text[91]

Often the number of integrin receptors displayed on the cell surface does not correlate with expression levels of integrins since the production of α- and β-subunits may not be balanced. The pairing of integrin with their binding partners to form heterodimers occurs in the endoplasmic reticulum (ER), and only intact heterodimeric αβ integrins appear on the cellular surface [36].

In cells surface integrins can exist in different conformation that influence their activation status (Figure 5):

- **inactive**, when the structure is folded and has a low affinity for the ligands of the ECM;
- **intermediate**, when the structure is relaxed but is not yet related to the ligand;
- **active**, when the conformational modification is completed, making the structure more similar to the ECM ligand.

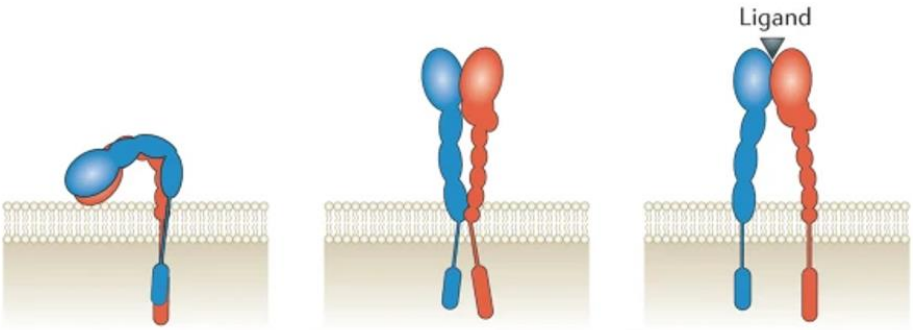

Affinity	Low	Intermediate	High
Conformation	Bent	Extended	Open
Outside-in signalling	No	No	Yes

Figure 5: Integrins conformational changes. The bent or inactive (left), extended or intermediate (middle) and extended-openor active (right) conformations β integrins. The α subunit is shown in blue, and the β subunit is shown in red. The ligand-binding site is indicated by a grey triangle in the extended-open integrin. Modified from *Ley, K., Rivera-Nieves, J., Sandborn, W.* et al. 2016.

Integrins are unique when compared with other transmembrane (TM) receptors in their ability to signal bidirectionally. Integrating the extracellular and intracellular environments, they bind ligands outside the cell or signalling molecules and cytoskeletal components inside the cell. This bidirectional signalling influences the adhesiveness of integrins for their ligands via two mechanisms, namely 'inside–out' and 'outside–in' signalling.

Inside–out signalling involves an internal signal binding to the cytoplasmic tail of integrins. The signal promotes conformational changes in the heterodimer and influences the affinity of integrin for its ECM ligand. Both the TM domain and the cytoplasmic one play important role during integrins activation. The TM domains exist in a coiled-coil structure in the resting or inactive state maintaining separated α- and β-subunits in close proximity to reach the activate status (Figure 5). The function of the cytoplasmic tails during integrin activation is to facilitate the binding of integrin adaptor proteins, such as talin and kindling[37]. The protein adaptor binding facilitates the tails separation that destabilized the head facilitating the extended conformation. In this 'active' extended conformation with open headpiece, integrins are able to bind extracellular ligands[31]. Integrins conformation is also regulated by glycosylation modifications which contributes to integrins activation or inactivation[38]. The attachment of carbohydrate to the amide nitrogen of asparagine (Asn, N) residues, a process named N-linked glycosylation, is one of the most abundant post-translational modifications especially for integrins. It has been demonstrated that protein N-glycans play important roles in many cellular processes such as cell adhesion and migration by modulating the function of cell adhesion molecules[38].

Outside–in signalling involves integrin binding to ECM ligands to induce conformational changes first, followed by integrin clustering and the assembly of large intracellular adhesion complexes[39]. Protein tyrosine phosphorylation is an important event in outside–in signalling and is mediated mostly by Src and FAK family protein tyrosine kinases.

By binding to ECM proteins, integrins do not simply regulate adhesion, but also activate specific signalling pathways leading to tumour cell migration, invasion, proliferation and survival[40].

In addition to play a decisive role in biological processes such as cell differentiation, tissue morphogenesis and angiogenesis at the embryonic level, integrins are involved in numerous pathological events such as tumour cell invasion and metastasis, thrombosis and inflammation[41 42]. It has been observed that integrins undergo changes in their configuration at the membrane during neoplastic transformation[43].

The invasive ability of tumour cells depends on the integrins expressed on the cell surface. During metastatic dissemination, integrins play a fundamental role in the homing of cells in the "metastatic niche", since they mediate specific signals recognition between tumour cells and the surrounding ECM[44]. Moreover, in the context of drug resistance, recent studies have shown that adhesion proteins (CAMs), in particular integrins, play a key role for cancer cells in platinum-based chemotherapy resistance[45]. In particular cancer stem cells (CSCs) are considered the root of carcinoma relapse and drug resistance in ovarian cancer. Bioinformatics analysis identified CSCs signatures in drug-resistant cells. Upon 36-genes signature, some α subunit integrins (here after ITGA), ITGA1, ITGA5 and **ITGA6,** were found enriched in side population (SP) [46]. The SP cells share characteristics of CSCs, specifically, they are enriched for tumor initiating capacity, they express stem-like genes, and they are resistant to chemotherapeutic drugs. and also in drug resistant cells[47].

1.3 ITGA6 promoter, transcript splicing, structure and function.

ITGA6 is a transmembrane glycoprotein that belongs to the laminin receptor protein sub-family (PS1). The gene coding for ITGA6 (Gene ID: 3655) is located on chromosome 2 (2q31.1) with a total length of 78870 bp (http://atlasgeneticsoncology.org/Genes/GC_ITGA6.html). The ITGA6 **promoter** directs transcription from a primary site to 208 nucleotides from the translation start codon. It contains a TATA like sequence (GATAAA), corresponding to the TATA BOX sequence. There is a CpG region, a receptor site for glucocorticoids and progesterone, and putative binding sites for the transcription factors SP1, AP2 and c-MYC. Recent in vitro and in vivo studies have shown that c-MYC binds to the ITGA6 promoter and could either inhibit[48] and activate[49] it in a cell dependent context. Also SP1 seems to be essential for ITGA6 promoter activation [50]. After transcription, ITGA6 pre-mRNA could be alternatively spliced in two different isoforms: ITGA6A and ITGA6B. The

ITGA6A **transcript** consists of a 5′-untranslated region (146 nucleotides), an open reading frame (ORF; 3219 nucleotides), and a 3′-untranslated region (2264 nucleotides). The ORF encodes a putative signal peptide (23 amino acids), an extracellular domain (988 amino acids), a transmembrane region (26 amino acids), and a short cytoplasmic domain (36 amino acids). The alternatively **spliced form** (ITGA6B) is due to the skipping of the last exon that results in the deletion of the last 130 nucleotides of its coding region and in the elimination of the original stop codon. The producing the alternative splicing variant ITGA6B is the results of the translation of a portion of ITGA6 3' UTR region that is 18 amino acids longer than ITGA6A isoform[51]. Since the C-terminus of the ITGA6B isoform has a high number of charged amino acids (24 out of 54) it also has a slightly higher molecular weight (160kDa) respect to the ITGA6A isoform (140kDa) [51]. Except for the GFFKR sequence at the N-terminus of the cytoplasmic domain, common to all α-integrin subunits, the two ITGA6 isoforms have no sequence homology at the cytoplasmic domain, and therefore could activate different signals transduction pathways within the cell, although this possibility should be experimentally demonstrated in greater details. Several splicing factors were identified responsible for ITGA6 isoforms: epithelial splicing regulatory protein 1 and 2 (ESRP1 and ESRP2), RNA Binding Motif Protein 47 (RBM47), the RNA-binding protein Muscleblind (MBNL1) and the RNA-binding protein FOX2 homologue (RBFOX2) as well as the polypyrimidine tract-binding protein 1 (Ptbp1). Among them, the most described are the ESRPs. ESPR1 is known to promote exon skipping by binding to the consensus UGG-rich motif in either introns or exons. Mutations of the UGG motifs downstream of exon 25 in ITGA6 abolishes ESRP1 binding. Furthermore, loss of ESRP1-mediated mRNA splicing results in increased ITGA6B isoform. At the same time, knockdown of ESRP2 resulted in a decrease in ITGA6A and an increase in ITGA6B. Moreover, ESRPs regulate transcripts undergo splicing during the EMT[52]. Recent evidences suggest that, in colorectal cancer cells, c-MYC on one side positively regulates ITGA6 expression and on its splicing acting on the expression of the splicing factor ESRP2. In particular c-MYC results in ESRP2 depletion and in increase expression of ITGA6B [49]. This findings introduced c-MYC as ITGA6 regulator, not only for its splicing but also for its promoter activation[49].

A wide range of cells types **express** ITGA6: fibroblasts[32], endothelial cells[53], leukocytes, and epithelial cells[54]. ITGA6 is expressed in almost all normal and tumour epithelial cells and in mice ITGA6 knockout is lethal in the neonatal stage, due to severe blistering of skin and other epithelial tissues[55]. ITGA6 is considered a stem cell marker, being expressed in more than 30 stem cell populations, including pluripotent, multipotent and cancer cells[56], as well as in breast, prostate and colorectal cancer. In this context, the high expression of ITGA6 was significantly associated with poorer progression-free survival in 287 ovarian cancer patients of TCGA cohort.

Immunohistochemistry analysis were performed on a total of 54 ovarian cancer tissues (25 drug resistant and 29 drug sensitive tissues), indicated that ITGA6 was normally located in the cell membrane. The percentage of chemo-resistant cases expressing ITGA6 was 60.0%, but the expression of ITGA6 in chemo-sensitive tissues was 31.0%, indicating that the expression of ITGA6 was increased in chemo-resistant tissues. These EOC patients with high ITGA6 expression exhibited a poorer PFS and an OS, compared with patients exhibiting low ITGA6 expression[40].

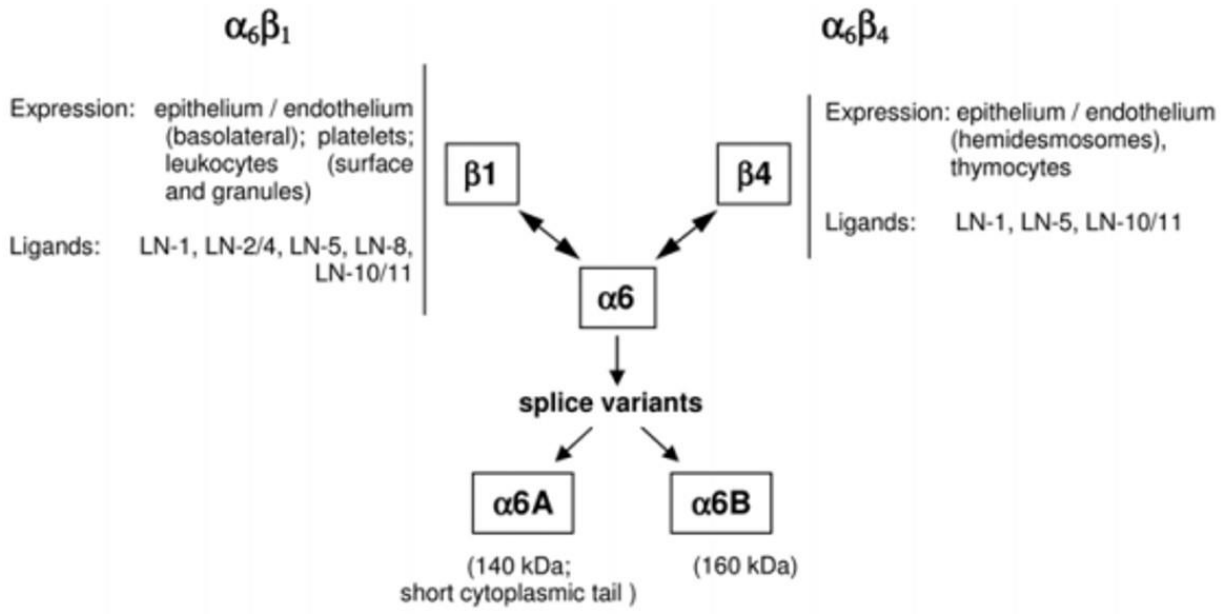

Figure 6: Summary of ITGA6 interactors and isoforms. The integrin A6 subunit can pair with both β1 and β4 subunits to form two distinct laminin binding integrins. The A6 gene encodes for two spliced variants named A6A and A6B with a variability in the length of their intracellular regions, 36 and 54 amino acids, respectively. Images takes from *Voisin MB., Nourshargh S. (2007).*

ITGA6 can be associated with the β1 or β4 subunits assuming different roles and functions[57]. **The α6β1 heterodimer** is generally present in leukocytes, platelets, lymphocytes and in epithelial stem cells, including undifferentiated human ESCs, where it is associated with maximum affinity to laminins. Precisely, the α6β1 association has been identified as a contributor to tumour spread, invasion and metastasis. Furthermore, this integrin is able to control the renewal and differentiation of stem cells[58], which need a specific microenvironment that provides signals for self-renewal and pluripotency.

The α6β4 association is mainly expressed in epithelial cells but also in a subgroup of endothelial cells[59], as well as from Schwann cells in peripheral nerves, platelets, macrophages and fibroblasts. Integrin α6β4 allows the formation of hemidesmosomes on the surface of the basal cells, or adhesive structures necessary to connect laminins of the basement membrane to the cytoskeleton of the

intermediate filament [60]. In the absence of the α6β4 heterodimer, the hemidesmosomes would fail, causing the loss of epithelial integrity, resulting in cell death. This heterodimer has also been associated with an aggressive and invasive carcinoma phenotype[61] playing important roles in tumour progression via activation of phosphatidylinositol-3 kinase signalling, promoting invasion and migration in breast cancer [62].

More recently it has been proposed that ITGA6 **isoforms might have different functions** in the cell signalling. In breast cancer the epithelial population predominantly expresses ITGA6A(β1), whereas the mesenchymal population predominantly expresses ITGA6B(β1)[63]. In contrast, undifferentiated human intestinal cells predominantly express ITGA6A(β4), whereas ITGA6B(β4) expression is mainly detected in differentiated cells[64]. The cytoplasmic domains of both ITGA6A and ITGA6B contain serine, threonine, and tyrosine residues, which could serve as potential phosphorylation sites. In fact it has been demonstrated that during adhesion on laminin ITGA6 is phosphorylated in its cytoplasmic domain. The latter contains three amino acids (SDA) in ITGA6A that are a typical PDZ-binding motif, whereas the corresponding amino acids (SYS) in the cytoplasmic tail of ITGA6B represent an alternative PDZ-binding motif. The SYS motif in ITGA6B is less efficient in binding to the signal molecules than the SDA motif in ITGA6A, and it may mediate differential intracellular signals[65]. In Breast cancer it was found that ITGA6A(β1), but not ITGA6B(β1), was responsible for protein kinase C–dependent activation of MAP kinases. ITGA6A(β1) was also found to be more active than A6B(β1) in promoting migration of bone marrow stem cells. On the other side, it is described that CSCs produce a laminin (LM) 511 matrix that promotes self-renewal and tumour initiation by engaging the ITGA6Bβ1 integrin and activating the Hippo transducer TAZ. In turn, TAZ regulates the transcription of the α5 subunit of LM511 and the formation of a LM511 matrix. These data establish a positive feedback loop involving TAZ, LM511 and ITGA6Bβ1[66].

All these data, somehow controversial depending on the models used, strongly support the possibility that the alternative splicing of ITGA6 plays a role in cancer progression and indubitably call for more compelling analyses.

2. AIM OF THE THESIS

Emergence of PT-resistant clones under the pressure of chemotherapy represents a frequent event for EOC that greatly hampers therapeutic success.

Primary advanced and relapsed EOCs are characterized by peritoneal dissemination and carcinosis. This is a peculiar type of metastatic dissemination, in which EOC cells shed from their site of origin, survive as cell clusters/spheroids within the abdominal cavity, and then root and thrive on the mesothelial cell lining of peritoneal cavity organs. Shed EOC cells or spheroids interact with the mesothelial lining by engaging specific cell-cell and cell-matrix adhesion molecules, such as integrins. How the acquisition of a platinum (PT)-resistant phenotype also contributes to the ability of EOC cells to spread and grow on the peritoneum through specific integrin-ECM interactions is still not clearly demonstrated. Therefore, in this PhD project, using isogenic PT-resistant EOC cells as a model, we aimed to study the role of integrins as a novel therapeutic target to avoid the invasion process in EOC cells. Based on FACS analyses evaluating integrins expression in parental and PT-res clones, we focused our studies on integrin alpha 6 (ITGA6), the most commonly overexpressed integrin in our PT-res models. Therefore, we dissected the role of ITGA6 in mediating EOC spreading both *in vitro* and *in vivo*. To this purpose, we used both genetic (CRISPR/Cas9 technology) and "pharmacological" (specific blocking antibody) approach to better characterize the molecular mechanisms underlying ITGA6 activity on PT-response, spheroids formation, invasion and adhesion. Overall, we demonstrated that targeting ITGA6 is a pursuable anticancer strategy to improve low survival of patients with PT-resistant diseases.

3. MATERIAL AND METHODS

3.1 CELL COLTURE

TOV-112D (CRL-11731) and OVSAHO (JCRB1046) cells were obtained from the American Type Culture Collection (ATCC) and the JCRB Cell Bank respectively. All these cell lines were maintained in RPMI 1640 medium (Sigma-Aldrich) supplemented with 10% heat-inactivated fetal bovine serum and 1% penicillin/streptomycin. All cell lines were grown in standard conditions at 37°C and 5% CO2 and routinely authenticated in our laboratory using the Cell ID TM System (Promega) protocol and using GeneMapper ID version 3.2.1 to identify DNA short tandem repeat profiles (last authentication was on 29 May 2018). Cisplatin-resistant (PT-res) isogenic cells were generated by treating EOC parental cells for growth for 2 hours with a cisplatin dose 10-fold higher than the calculated IC50 and then allowing to re-grow in drug-free complete medium (pulse treatment). The subsequent drug treatment was administrated when the cells reached again a 70-80% of confluence. In total PT-res cells received 20 pulse treatments. At the end of treatments, a single cell cloning was performed in order to evaluate the homogeneity of these PT-res cell populations. The cisplatin IC50 of clones was tested.

3.2 FLOW CYTOMETRY

Cells were grown in 100 mm tissue culture plates to 90-95% confluence and harvested with 5mM EDTA. Cells were incubated with primary antibodies PE anti CD49f, APC anti CD49c, PE anti CD49e; PE anti CD29, PE anti CD104 from BD Pharmingen for 15 minutes at 4°C, washed three times with ice-cold 1% BSA/PBS buffer. Cells were re-suspended in 0.3 ml of ice-cold 1% BSA/2mM EDTA in PBS buffer and kept on ice. Flow cytometry was performed using FACs LSFortessa(BD Bioscience) and data were analysed using DIVA software (BD Bioscience). Isotype-matched antibodies were used as controls.

3.3 GENERATION OF ITGA6 KO WITH CRISPR TECHNOLOGY

The following protocol was adapted from Ran et al. [67]. Two guide RNAs (gRNAs) were designed using the CRISPR Design online tool (https://zlab.bio/guide-design-resources) to target the exon of ITGA6 (NC_000001.11) sequences of the two gRNAs as in Table 1

The pairs of annealed oligonucleotides were cloned in the gRNA expression vector pSpCas9(BB)-2A-GFP plasmid (pX458, Addgene #48138) (www.addgene.org/). We transfected 2 μg of this plasmid in the TOV-112D AND OVSAHO PT-res cells line with Lipofectamine 2000 according to the manufacturer's protocol. Seventy-two hours after transfection, GFP-positive cells were sorted by flow cytometry (Becton Dickinson) and pooled together. To confirm the presence of mutations surrounding gRNA target sites, we purified and sequenced the genomic DNA from the TOV-112D AND OVSAHO pool cells. By these means, we identified mutations around the predicted point of double-strand breaks. Pooled cells were seeded as single colonies (0.5 cells per well) in ten 96-well

plates. After 2 to 3 weeks of expansion, the cells in each colony were divided in half; one half was subjected to propagation and the other half was used to assess the expression of ITGA6 using Western blot analysis. The genomic DNAs of clones showing a consistent reduction in ITGA6 expression were analyzed using a MiSeq instrument (Illumina) to confirm the presence and exact allelic fraction of mutations. We only used clones where we detected 100% allelic frequency.

3.4 CELL VIABILITY AND DRUGS COMPOUNDS

Dose-response curves were performed essentially as described previously [68]. Briefly, epithelial OC (EOC) cells were seeded in 96-well culture plates coated or not with 1% Matrigel and treated with CDDP (TEVA Italia) for 72 hours at 37°C at the indicated concentrations. Cell viability was determined 72 hours after treatment using the CellTiter 96 AQueous cell proliferation assay (MTS)(Promega). For treatment with SP1 inhibitors mithramycin (Sigma-Aldrich) was used at 0,5 µM at different time point. The specific MYC-MAX inhibitor 10058-f4 (Sigma-Aldrich, F3680) was used at 10µM. All the inhibitors were dissolved in DMSO and stored at -20°C. The specific N-glycosylation inhibitor (Tunycamycin, Sigma-Aldrich readymade solution) was used at 1µM. ITGA6 and SNAIL protein stability was evaluated by treating (or not) with CHX (10 µg/ml) or with MG-132 (10 µM) for the time indicated.

3.5 ADHESION ASSAY

The quantitative cell adhesion assay was performed using the CAFCA quantitative adhesion methods[69]. On 6-well strips of flexible polyvinyl chloride coated with 10 µg/ml Laminin 511 (LN10). Cells were labelled with the vital fluorochrome calcein acetoxymethyl (Invitrogen) for 15 min at 37°C and then dispensed into the bottom CAFCA miniplates, which were centrifuged to synchronize the contact of the cells with the substrate. The miniplates were then incubated for 20 min at 37°C and were subsequently mounted together with a similar CAFCA miniplate to create communicating chambers for subsequent reverse centrifugation. The relative number of cells bound to the substrate and cells that failed to bind to the substrate was estimated by top/bottom fluorescence detection in a computer-interfaced Infinite M1000 PRO microplate reader (Tecan Group Ltd.).

3.6 EOC ADHESION ON MESOTHELIAL CELLS AND IMMUNOFLUORESCENCE ANALYSIS

Mesothelial cells (LPL) (derived from pleural lavage) were seeded on glass coverslips and allowed to grow until they reached complete confluence. 1.5×10^5 EOC cells detached with 5 mM EDTA, labeled with vital green fluorescent lipophilic tracer DiO (Invitrogen) and washed with PBS were then plated on mesothelial layer in serum free medium for 24 hours. For immunofluorescence analyses cells plated on coverslips were fixed in PBS-4% paraformaldehyde (PFA) at room

temperature (RT), blocked in PBS-1% bovine serum albumin (BSA). Then samples were washed in PBS and incubated with secondary antibodies (Alexa-Fluor 488-, 633- or 546-conjugated anti-mouse or anti-rabbit antibodies; Invitrogen) for 1 hour at RT. PI (5 μg/ml + RNaseA) or TO-PRO-3 iodide (Invitrogen) were used to visualize nuclei and Alexa-Fluor 647- or 546-Phalloidin (Invitrogen) for F-actin staining. Coverslips were mounted with glycerol/0.25% DABCO and analyzed using a the Leica Time Lapse AF6000LX workstation, the TCS-SP2 or the TCS-SP8 Confocal Systems (Leica Microsystems Heidelberg GmbH) interfaced with the Leica Confocal Software (LCS) or the Leica Application Suite (LAS) software.

3.7 EVASION ASSAY

For Evasion assays, 7.5×10^3 TOV-112D or OVSAHO EOC cells were included in Matrigel (Cultrex, BME) drops at a final concentration of 8 mg/ml (12 μl of matrix volume per drop). Matrigel was diluted in RPMI 1640 and 0.1% BSA. The drops, were dispensed in cell culture dishes and maintained for 1 hour at 37°C upside down to jellify. Then, the dishes were turned up, and the drops were incubated in complete medium. The evasion ability was evaluated 6 days after inclusion by measuring the distance covered by crystal violet–stained cells exiting from the drops (five drops/cell lines per experiment). Images were collected using a stereo microscope Leica M205FA.

3.8 SPHERE FORMING ABILITY

To establish primary spheres, cells were plated ($8x10^3$) on poly-HEMA coated dishes as single cell suspension in sphere medium containing phenol red-free DMEM/F12 (GIBCO), B27 supplement (50x, no vitamin A; Life Technologies), recombinant epidermal growth factor (hEGF, 20 ng/ml; SIGMA) and recombinant basic fibroblast growth factor (bFGF 20ng/ml). In a subset of experiments, CDDP was added to the medium as indicated. After 8-10 days, primary spheres were counted and sphere area was measured with ImagJ program.

3.9 PREPARATION OF CONDITIONED MEDIUM AND GROWTH ON MESOTHELIAL CELLS

For detection of extracellular ITGA6, confluent parental and PT-res WT or KO EOC cells were cultured for 24 h in serum-free medium in presence or absence of CDDP at different time point. Conditioned Medium (CM) from the cell lines were harvested and precipitated by the addition of TritonX-100 and trichloracetic acid (TCA). Equal amounts of proteins mixed with Laemmli buffer, separated in 4%–20% SDS-PAGE (Criterion Precast Gel, Biorad) and blotted onto a nitrocellulose membrane. For adhesion assay on mesothelial cells, we performed two types of experiments. In the first one, LPL were plated at confluence in 24 well plate. After 24 hours, they were challenged or not with CM from ITGA6 WT or KO cells for 16h in triplicate, after the removal of CMs, TOV-112D

parental cells (50.000) were plated on the conditioned LPL in normal media and leave to growth for 10 days. In the second experiment, CM from ITGA6 WT or KO cells were used to challenge TOV-112D parental for 16h. After treatment with CM, TOV112D cells were plated on not conditioned LPL monolayer and leave to growth for 10 days. For both experiments, we evaluated TOV-112D parental sphere forming ability, as described in the previous point.

3.10 PREPARATION OF ASCITES AND CONDITIONING ON MESOTHELIAL CELLS

Ascites were obtained from patients with epithelial ovarian cancer at different stages, cells were removed from ascites by centrifugation. Ascites were collected and filtered reducing the size of the filter mesh (45µM and 22 µM), then they were conserved at -80°C (Table 1 for the ascites). Cells were collected from ascites and lysate (Table 2). LPL were plated at confluence in 24 well plate After 24 hours, they were challenged or not with 2% of patients ascites samples (Table 1) in serum-free medium for 16h. GoH3 (2,5 µg/ml) was added to the medium during the 16h with the ascites. After 16h, the ascites +/- GoH3 were removed and TOV-112D parental cells (50.000) were plated on the conditioned LPL in normal media and leave to growth for 10 days. We evaluated TOV-112D parental sphere forming ability, as described in the previous point.

Table 1: Ascites Samples

Patients Number	Age	Tumour Histotype	Stage
1	82	HGSOC	IV
2	69	HGSOC	IV
3	87	uterine carcinosarcoma	na
4	59	HGSOC	Na
5	71	HGSOC	IIIC
6	73	HGCCOC	IVB

Table 2: Cells extracted from ascites

Patients Number	Age	Tumour Histotype	Stage
1	63	HGSOC	IV
2	63	MUCINUS	IV
3	53	HGSOC	T3C

4	65	HGSOC	T3C
5	82	HGSOC	IV
6	50	HGSOC	T3C
7	50	HGSOC	T3C
8	62	HGSOC	T2

3.11 LUCIFERASE ASSAY

Luciferase assay was performed to validate c-MYC and SP1 putative target sites on ITGA6 promoter. Briefly, the sequence of ITGA6 promoter was amplified from genomic DNA of TOV-112D cells using specific primers. PCR product was first subcloned in the pGEM-T easy vector (Promega) and then digested with XhoI and BamHI restriction enzymes to be cloned in the pGL3-basic vector (Promega) at the 5' of the luciferase gene. For luciferase assays, TOV-112D cells were co-transfected with 500 ng of pGL3 reporter construct bearing the ITGA6 promoter and 50 ng of pRL Renilla Luciferase Control Reporter (RL-TK) (Promega) vector in combination with pCMV-c-MYC (Addgene #40900) or RSV-Sp1 (Addgene #12098) and an empty vector (pEGFP-C1 or pCMV, Clontech) in 24-well plate using FuGENE® HD Transfection Reagent (Promega). After 48 hours from transfection, cell lysates were assayed for luciferase activity using the Dual-Luciferase reporter assay system (Promega) according to manufacturer's recommendations. Values were normalized using Renilla luciferase.

3.12 ELISA

20µl of ascites were diluted in 180 µl of PBS 1x and ITGA6 levels from patients ascites samples (Table 2) were detected using commercially available ELISA kit (MyBioSource) following the manufacturer's protocol.

3.13 HUMAN RECEPTOR TYROSINE KINASE PHOSPHORYLATION ANTIBODY ARRAY

For the human receptor tyrosine kinase (RTK) phosphorylation antibody (Ab) array (RayBiotech Inc., Norcross, GA), TOV-112D PT-res WT vs KO have been adhered on laminin for 30 min or 1h and protein lysate were collected. Then the lysate were incubated with the array membrane and protein signal was visualized using a chemifluorescence detection system (Bio-Rad, Hercules, CA), according to the manufacturer's protocol. Relative density of specific protein expression was determined using ImageLab software.

3.14 PREPARATION OF LAMININ COATING, CELL LYSATES AND IMMUNOBLOTTING

Coated plate were prepared using Laminin 511 (Matrixome) 5µg/ml diluted in Carbonate Buffer pH 9.8. The plate were leaved for 1h at 37°C or overnight at 4°C then aspirated the cover solution and immediately seed the cells. Cell lysates were prepared using cold RIPA buffer [150 mM NaCl,50 mM tris-HCl (pH 8), 0.1% SDS, 1% Igepal, and 0.5% NP-40] containing protease inhibitor cocktail (Roche) phosphatase inhibitors1 Mm Na3VO4 and 10 mM NaF (Sigma-Aldrich) plus 1 mM DTT. Protein concentrations were determined using the Bio-Rad protein assay (Bio-Rad). Proteins were separated in 4 to 20% SDS–polyacrylamide gel electrophoresis (SDS-PAGE) (Criterion Precast Gel, Bio-Rad) and blotted onto a nitrocellulose membrane (Amersham, GE Healthcare). Membrane strips were blocked with 5% nonfat dried milk in tris-buffered saline (TBS)–0.1% Tween 20 or in Odyssey Blocking Buffer (LI-COR,Biosciences) and incubated at 4°C overnight with primary antibodies. The following primary antibodies were used: c-Myc (1:1000, #5605), SNAIL (1:1000, #3879), SLUG (1:1000, #9585), pERK (1:1000 #9101), pLYN Y507 (1:1000 #2731), LYN (1:1000 #2796), ZEB1 (1:1000 #3396), ZO1 (1:1000 #8193), were from Cell Signalling Technology; Vinculin (1:5000, sc-7649), c-Myc (1:500, sc-40), ERK (1:500, sc-271269) and TWIST (1:1000, sc-81417) were from Santa Cruz Biotechnology; ITGA6 (1:500 ,HPA01269) and SP1(1:500, SAB1404397) from Merk-Sigma, pFAK Y397 (1:500 44624G) from Invitrogen, FAK (1:500, F15020) from BD Transduction laboratories, pLYN Y397 (1:1000, ab226778) from Abcam and GAPDH (1:1000 CB1001) from Calbiochem. Antibodies were visualized with appropriate horseradish peroxidase (HRP)–conjugated secondary antibodies (GE Healthcare) for chemiluminescent detection (Clarity, Bio-Rad) or with Alexa-conjugated secondary antibodies (Invitrogen) for Odyssey infrared detection (LI-COR Biosciences).

3.15 RNA ISOLATION AND REAL-TIME POLYMERASE CHAIN REACTION

Total RNA for RNA microarray and qRT-PCR analyses was isolated from patient-derived primary tumors or cell cultures using Trizol solution (Roche Applied Science Mannheim, Germany) according to manufacturer protocol. Total RNA was quantified using NanoDrop (Thermo Fisher Scientific Inc., USA). 1ug of RNA was retro-transcribed with GoScript reverse transcriptase to obtain cDNAs, according to provider's instruction (Promega). Absolute quantification was evaluated by qRT-PCR, using EvaGreen dye-containing reaction buffer (SsoFastTM EvaGreen®, BioRad) and running the reactions in the CFX384 (Biorad) Two Color Real-time PCR Detection System (Biorad). Data normalization was performed using ACTIN as housekeeping genes and relative expression was

calculated using the mRNA concentration. All the primers for gene expression analyses were purchased from Sigma-Aldrich. Table 3 below reports all the primer sequences.

Table 3: Primer

Gene	Primer Forward 5'-3'	Primer Reverse 5'-3'
ITGA6	AAGTCTCGTTCCTGTTCCTGC	ACTGTGATTGGCTCTGGGAG
ITGA6A	GAGATCCATGCTCAGCCATC	ACTGTCATCGTACCTAGAGCGTTT
ITGA6B	ACTATGGAAGTGTGGATTCTTT	CCCCCGCTATGAGTAGCTTT
ACTIN	CCAGAGGCGTACAGGGATAG	CCAACCGCGAGAAGATGA
SP1	GGTGCCTTTTCACAGGCTC	CATTGGGTGACTCAATTCTGCT
MYC	CTCCTGGCAAAAGGTCAGAG	TCGGTTGTTGCTGATCTGTC
ESRP1	GGGAGTTCGCCACAGATATTC	AGCCATAAATGCTCTGTCCG
ESRP2	ATGGCACAGGGTTTAGGAC	TTTCTGCTTTATCACCTCGGG
ITGA6 PROMOTER	CTCGAGTTTTGAGGGTTGTTAGG	AGATCTGGGTCGCCGCTCTCCGTC
ITGA6 for ChIP	TTGTGTACATTATACAGCAC	GGAGACTTTACTACCCGTTATAAA
gRNA ITGA6 3	GGGCTGCAGTTGCCAGTGCA	TGCACTGGCAACTGCAGCCC
gRNA ITGA6 2	AGAAGCCGAAGAGGCTCCCG	CGGGAGCCTCTTCGGCTTCT

3.16 CHROMATIN IMMUNOPRECIPITATION ASSAY (ChIP).

TOV-112D cells was crosslinked with 1% formaldehyde and chromatin was prepared *via* MNase enzymatic digestion according to the protocol. Chromatin immunoprecipitation (IP) was performed using SimpleChIP Enzymatic Chromatin IP kit - Magnetic Beads (#9003, Cell Signaling Technology). After IPs, DNA was purified and analyzed by qRT-PCR (see above). Results were reported as ITGA6 promoter enrichment of putative ITGA6 promoter fragment (SQ mean) folded on unrelated IP (control IgG) as described in Dall'Acqua et al, 2017 [70] using the primer in Table 1.

3.17 PATIENT'S CLINICAL DATA

EOC patients' plasma samples were collected at the Centro di Riferimento Oncologico (CRO) Aviano, National Cancer Institute between 2014 and 2017 from patients who signed an informed consent form. This prospective observational clinical trial was approved by the Internal Review Board

(IRB) (protocol no. CRO-IRB 05-2014). From each enrolled EOC patient, we collected one blood sample before the chemotherapy (baseline, I sample) and one sample at the end chemotherapy (II sample). Patients' baseline characteristics are summarized in Table 2. Tumor staging was in accordance with the International Federation of Gynecology and Obstetrics (FIGO) criteria. Patients were followed for at least two years to verify the effect of biological and clinical-pathological characteristics on overall survival (OS). OS was defined as the time interval in months between the time of surgery and the date of death for non-censored events or until the date of last contact for censored events when the woman was still alive.

List of stage III–IV EOC patients included in Table 4 below reports the pathological variables of patients included in this study and described in Figure 6C–E. * HGSOC = high grade serous ovarian cancer. LGSOC = low grade serous ovarian cancer.

Table 4: Serum samples

Patient Number	Age	Tumor Histotype *	Tumor Stage
1	67	HGSOC	IV
2	55	HGSOC	IIIC
3	72	HGSOC	IV
4	57	HGSOC	IV
5	70	HGSOC	IV
6	54	HGSOC	IIIC
7	69	HGSOC	IV
8	43	HGSOC	IV
9	82	HGSOC	IIIC
10	36	LGSOC	IV
11	81	HGSOC	IIIC
12	64	HGSOC	IIIC
13	72	HGSOC	IIIC
14	68	HGSOC	IIIC
15	70	HGSOC	IIIC
16	41	HGSOC	IIIC
17	57	HGSOC	IIIC
18	65	HGSOC	IV
19	67	HGSOC	IV
20	82	HGSOC	IIIC
21	56	HGSOC	IIIC

3.18 IN VIVO TUMOUR XENOGRAPH

Animal experimentation was reviewed and approved by the Centro di Riferimento Oncologico di Aviano (CRO) Institutional Organism for Animal Wellbeing (OPBA) and by the Italian Ministry of Health (authorization no.1261/2015-PR released to Dr. Gustavo Baldassarre). All animal experiments

were conducted in adherence to international and institutional committees' ethical guidelines. Female NOD scid gamma mice (NSG) (4 weeks old) were acquired from Charles River Laboratories and xenografted with 2×10^6 ITGA6 WT and KO TOV-112D cells intraperitoneally in sterile phosphate-buffered saline. After 30 days from injection (in accordance with our previous observations of intraperitoneal injection of the same cells), animals were sacrificed. Dissemination was recorded and annotated by photographs and charted on the basis of organ dissemination. Tissues were fixed in 4% paraformaldehyde before dehydration in ethanol and xylene before paraffin embedding and then stained with hematoxylin and eosin.

3.19 STATISTICAL ANALYSIS

Graphs and data analyses were carried out utilizing PRISM software (version 6, GraphPad, Inc.). Where the means of two data sets were compared, and significance was determined by a two-tailed Students t-test or ANOVA, as indicated in each figure. Differences was considered significant at $p < 0.05$ (* $p \leq 0.05$, ** $p \leq 0.01$, *** $p \leq 0.001$, **** $p \leq 0.0001$).

4. RESULTS

4.1 ITGA6 is commonly overexpressed in PT-res cells. Few models of isogenic ovarian cancer platinum resistant cell (PT-res) lines exist to properly study molecular alterations induced by PT-resistance in EOC. To better address this issue in our lab we have established 7 different PT-resistant cell lines encompassing all the histological subtypes, using two methods: the increasing dose method and the pulse one as described in Sonego et al. [68]. The first three PT-res models (MDAH-2774, TOV-112D and OVSAHO) have been characterized [71]. Respect to their parental (sensitive) counterpart, PT-res cells display: higher cisplatin IC50, decreased PT-induced of DNA damage and faster restoration of the PT-induced S phase block [68]. Another aspect shared among all PT-res cells was a visible alteration of their morphology. These morphological modifications suggested that the balance between epithelial and mesenchymal status (epithelial-mesenchymal transition, EMT) was altered in PT-res cells, conferring a more invasive phenotype. Accordingly, PT-res cells better adhered on mesothelial cells monolayer, in vitro[68].

In this PhD project, we dissected the molecular mechanisms underlying the higher adhesion ability of PT-res EOC cells. Cell adhesion to Extra Cellular Matrix (ECM) and mesothelial cells layer is mainly mediated by specific surface receptors called Integrins that function as heterodimers composed by an α and a β subunit [72]. To address whether increased cell adhesion could be correlated with alterations in integrins expression, FACS analysis was used to investigate the cell surface expression of the integrin subunits β1, β3, β4, α1, α2, α5, α6 and αv in TOV-112D and OVSAHO Parental and PT-res pools (Figure 1a) accepted models of high grade endometrioid and high grade serous EOC, respectively. This analysis showed that Integrin α6, hereafter ITGA6, was the only integrin over expressed in all PT-res pools, respect to the parental counterpart. These data were further confirmed on single PT-res cell clones derived from TOV-112D and OVSAHO PT-res pools. All clones used were confirmed to be PT-resistant (Figure 1b) and expressed higher ITGA6 protein levels, as evidenced by western blot analysis (Figure 1c). Interestingly, in western blot analysis all tested PT-res cells clones overexpressed two ITGA6 bands of slightly different molecular wight (Figure 1c). Cells treatment with the potent N-glycosylation inhibitor Tunycamycin (TM), abrogated the expression of the ITGA6 protein upper band t (Figure 1d), suggesting that ITGA6 in PT-res is not only more expressed but also differently glycosylated. Since glycosylation of Integrins α subunits regulates their binding to the β subunits and integrins activations, this observation also suggests that ITGA6 could be differently actives in in parental and PT-Res cells.

ITGA6 functions primarily as receptor for laminins (LM), ECM components predominantly found in the basement membranes [73]. Based on this notion, we tested the adhesion ability of our models to LM10 used as substrate, being this LM isoform the most expressed in ovarian carcinoma[74]. Adhesion experiments showed that the adhesion of all tested PT-res clones was 10-20 fold higher than the

matched parental cells (Figure 2a). Moreover, using a specific anti-ITGA6 blocking antibody (hereafter GoH3), we confirmed that the higher adhesion of PT-res cells to LM10 was principally mediated by ITGA6 (Figure 2b). More importantly, all tested clones had a higher ability to adhere to the mesothelial cell layer and also in this case the adhesion was mainly mediated by ITGA6 (Figure 2c). Overall, these results support the idea that PT-res EOC cells commonly overexpressed ITGA6 that in turn conferred to these cells a greater ability to adhere and grow on mesothelial cells.

a

TOV-112D	ITGA1	ITGA2	ITGA5	ITGA6	ITGAV	ITGB1	ITGB3	ITGB4
Parental	0	0	100	10	83	100	0	0
PT-res pool#1	0	0	100	76	86	100	14	5
PT-res pool#2	0	0	100	71	89	100	4	2

OVSAHO	ITGA1	ITGA2	ITGA5	ITGA6	ITGAV	ITGB1	ITGB3	ITGB4
Parental	0	64	6	2	12	2	0	0
PT-res pool#1	0	89	10	11	9	2	0	0
PT-res pool#2	0	85	58	66	36	6	3	6

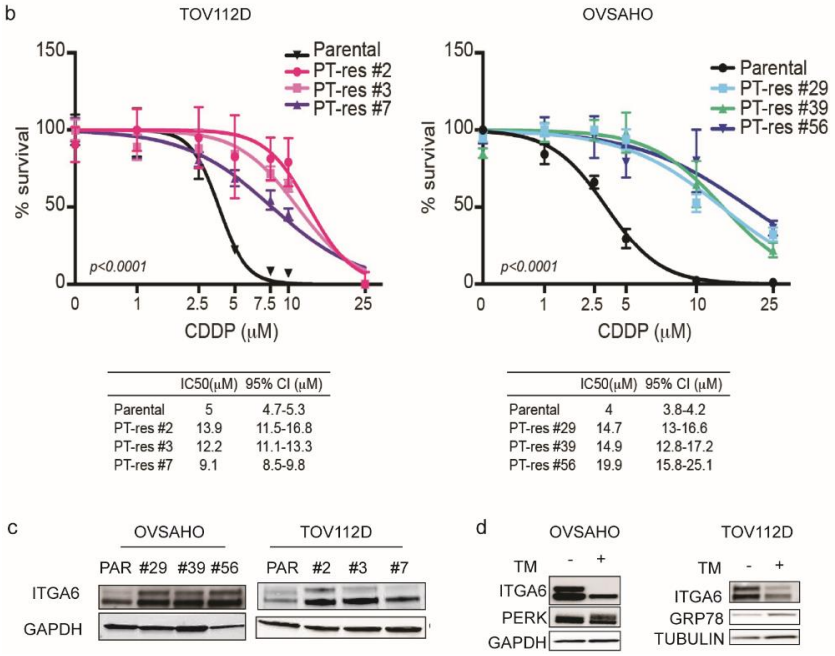

Figure 7: PT-res integrins characterization. (**a**) Tables reporting the percentage of integrins α and β positive cells in EOC parental and PT res pools (#1 and #2) TOV-112D and OVSAHO analysed by flow cytometry (FACS), using anti-ITGA1, ITGA2, ITGA5, ITGA6, ITGAV, ITGAB1, ITGAB3, ITGAB4, as describe in material and methods. Isotype-matched irrelevant antibodies were used as controls. One of three representative experiments is shown. (**b**) Nonlinear regression analyses of cell viability assay. TOV-112D and OVSAHO cells, compare with their PT-res counterpart, were treated with increasing doses of CDDP for 72 hours. Data are expressed as percentage of viable cells with respect to the untreated cells and represent the mean (±SD) of three biological replicates. The table shows the IC50 and the CI of each condition. (**c**) Western blot analysis of ITGA6 expression in TOV-112D and OVSAHO parental and PT-res. (**d**) ITGA6 expression level in PT-res cells treated or not with Tunycamycin (TM). For **d** and **c** Glyceraldehyde-3-phosphate dehydrogenase (GAPDH) and TUBULIN were used as a loading control.

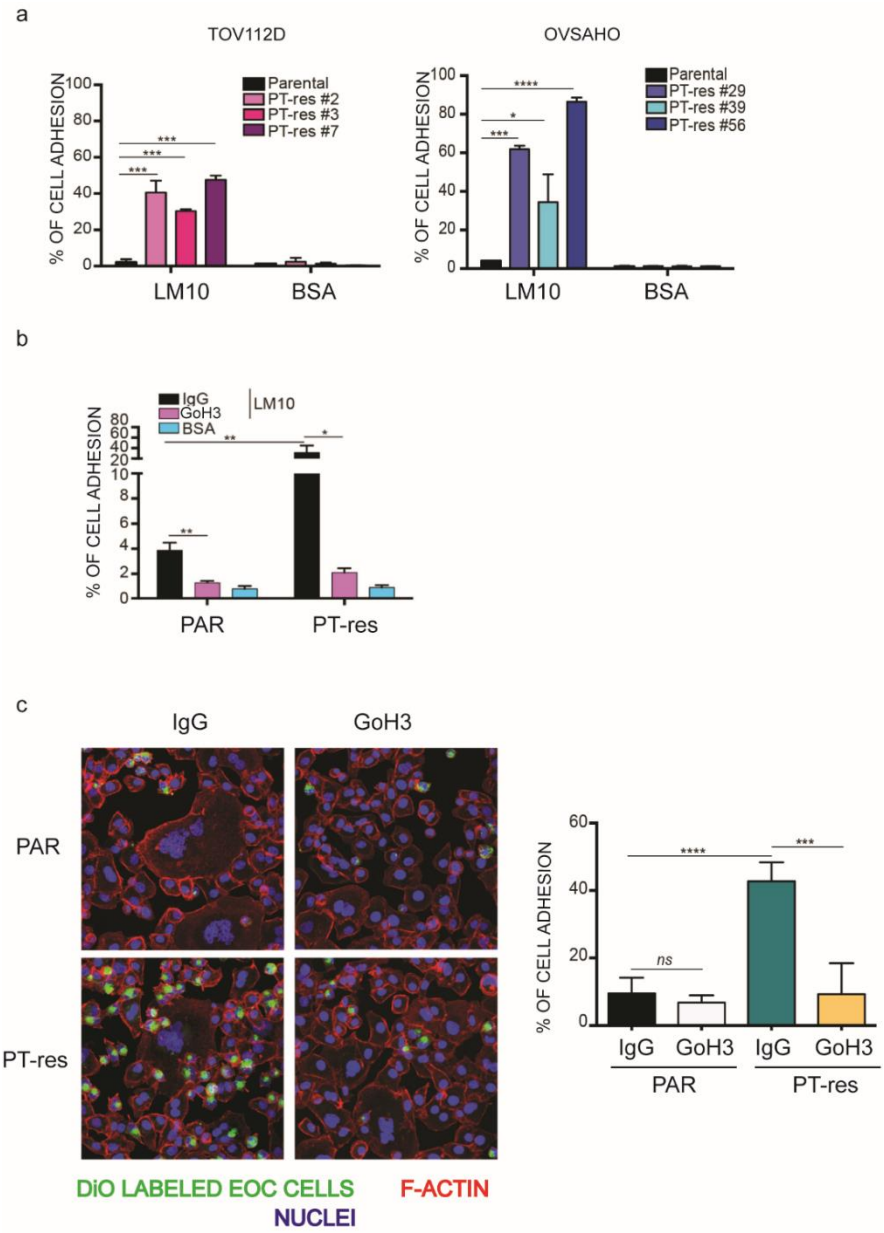

Figure 8: ITGA6 blocking antibody effects (**a**) The graphs represent the percentage of cells that adhere on LM10 monolayer, BSA was used as negative control. Number of cell adhesion was detected by a Fluorescence-base assay (as described in Methods section). (**b**) The graph shows the percentage of cells, TOV-112D, that adhere on LM10 in presence or not of a blocking antibody for ITGA6, GoH3 (as described in Methods section). BSA was used as negative control. (**c**) Maximal projections of images of parental and PT-res cells labeled with the green fluorescent marker DiO (green) and cultured on a monolayer of mesothelial cells for 24h, in presence or not of ITGA6 blocking antibody. Cells were then fixed and stained with Phalloidin (F-Actin, red) and TO-PRO3 (nuclei, blue). In the right graph, the number (mean ± SD) of cancer cells/field is reported. In the a, b and c figures, statistical significance was determined by a two-tailed, unpaired Student's t-test (*$p < 0.05$ and **$p < 0.01$)

4.2 ITGA6 is involved in PT-resistance, adhesion, spheres formation and evasion. To properly characterize the role of ITGA6 in PT-Res cells we generated ITGA6 knockout (KO) TOV-112D and OVSAHO PT-res cells using the CRISPR-Cas9 technology (Figure 3a). Again, we observed that the TOV-112D PT-res ITGA6-KO cells failed to adhere to LM10 when compared to ITGA6 WT PT-res cells (Figure 3b). This result confirmed that ITGA6 drives the adhesion of our PT-res cells.

To understand if ITGA6 also had a direct role on PT-res cells response to platinum (CDDP) we used kill curve analyses to evaluate the CDDP IC50 in parental, PT-Res and PT-res ITGA6 KO cells. ITGA6 knock out only slightly affected the CDDP IC50 of PT-res cells grown on plastic but significantly reduced CDDP IC50 when the cells were cultured on Matrigel coated dishes (Figure 3c), suggesting that adhesion to ECM contributed to confer resistance to CDDP of EOC cells and that this effect is at least partially mediated by ITGA6 engagement.

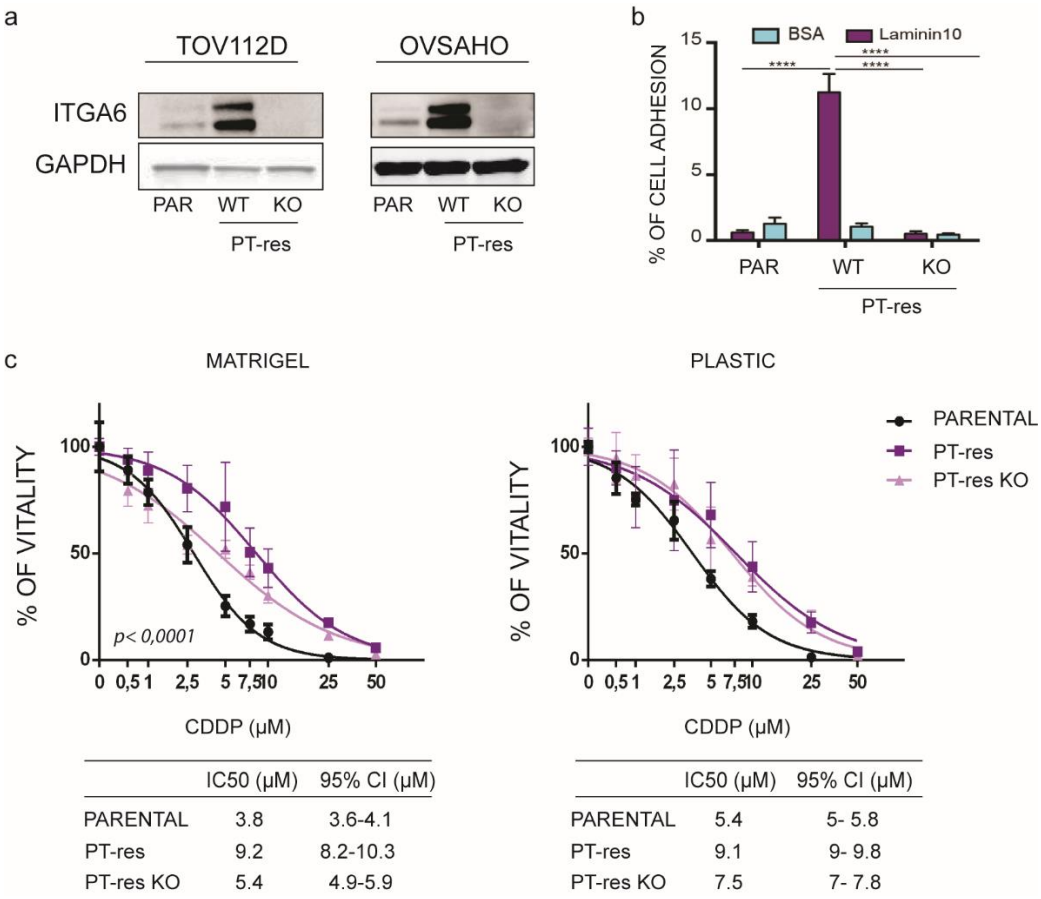

Figure 9: Adhesion ability and survival to CDDP of ITGA6 KO cells (**a**) Western blot analysis of ITGA6 expression in TOV-112D and OVSAHO parental and PT-res WT and KO. GAPDH was used as a loading control. (**b**) The graphs represent the percentage of cells that adhere on LM10 monolayer, BSA was used as negative control. The adhesion ability of TOV-112D PT-res KO#3 and #15 were compare with the parental and PT-res WT. Number of cell adhesion was detected by a Fluorescence-base assay as described in Material and Methods. (**c**) Nonlinear regression analyses of cell viability assay in TOV-112D parental cells, PT-res and PT-res KO #3. The cells were treated with increasing doses of CDDP for 72 hours, in not coated condition or coated with 0,5% of matrigel. Data are expressed as percentage of viable cells with respect to the untreated cells and represent the mean (±SD) of three biological replicates. The table shows the IC50 and the CI of each condition.

In accord with this possibility, some reports suggest that integrins in general and ITGA6 in particular, participate in the definition of a drug-resistant phenotype, possibly regulating their cancer stem-cell like (CSCs) subpopulation [75]. Sphere formation is an assay commonly used to evaluate cancer stem cell–like features in EOC models[76]. Using this assay on cells treated or not with CDDP we observed that in both TOV-112D and OVSHAO models we made several interesting information: 1) PT-res

cells formed CDDP insensitive spheres; ITGA6KO reduced the number and size of sphere formed by PT-res cells; 2) CDDP treatment had no effect on the sphere number and size formed by ITGA6KO PT-res cells; 3) Independently on their absolute number, sphere formed by parental cells sphere are extremely sensitive to CDDP treatment; 4) PT-res more than parental cells are sensitive to the pharmacological block of ITGA6 signalling with a specific blocking antibody (Figure 4a-d).

It is accepted that EOC dissemination in the abdomen and pelvis is due to the ability of ovaryspheres detached from the primary tumours to adhere and grow on mesothelial cells[77]. We thus examined the ability of spheres formed by TOV-112D Parental, PT-res ITGA6 WT and KO to adhere and grow on mesothelial cells monolayer for up to ten days. Data showed that PT-res WT forms more and bigger spheroids than both Parental and PT-res KO, which are more similar to the Parental condition (Figure 5a), supporting a role of ITGA6 in regulating the metastatic ability of PT-res cells. Since metastasis formation also relay on the ability of cells to move within a 3D matrix, we tested the motility of our cells included in Matrigel drops and allowed to exit from the matrix over a 5 days period. Parental cells have no (for TOV-112D) or very few (for OVSAHO) evasion events (Figure 5b and c), while PT-res WT cells of both cell lines efficiently evaded from the drops. Again, ITGA6 KO impaired this capability of PT-res cells (Figure 5b and c). Altogether these data support the involvement of ITGA6 in cells escape from the original tumour site, spheroids formation, spreading and then invasion of mesothelial substrate.

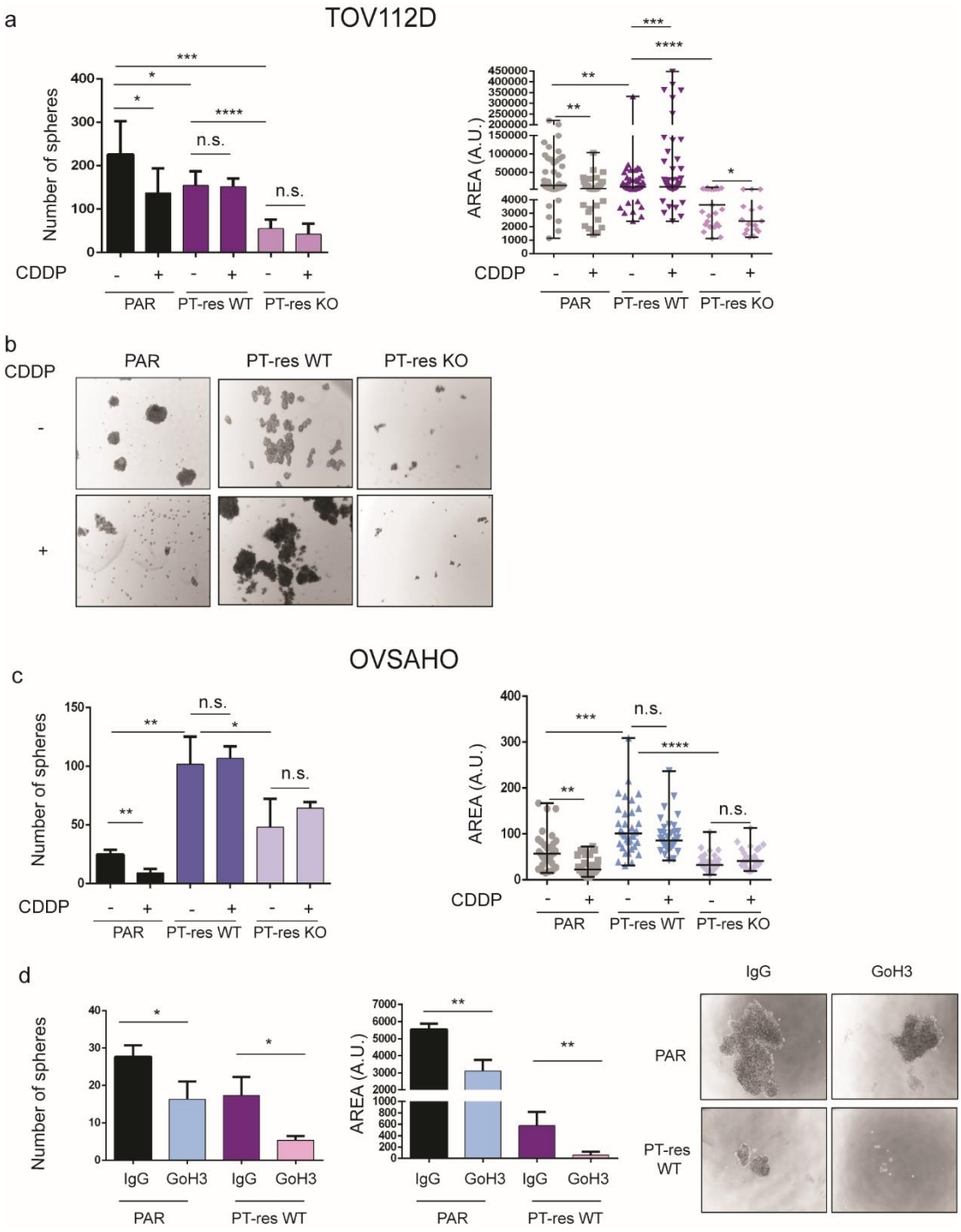

Figure 10: Sphere formation ability (**a**) Graph showing the ovarysphere-forming ability of TOV-112D Parental, PT-res WT and PT-res KO. CDDP (5µM) was added after 5 days and leave in for 5 days. Then area and number of spheres were measured. (**b**) Representative pictures of the TOV-112D experiment. (**c**) Graph represents the number (left) and area (right) of ovaryspheres of OVSAHO parental, PT-res WT and KO. CDDP (5µM) was added after 5 days and leave in for other 5 days. (**d**) The graph shows the number and the area of ovaryspheres with or without ITGA6 blocking antibody for TOV-112D Parental and PT-res. Representative image of the experiment are below. In both (**a**), (**c**) and (**d**) statistical significance was determined by a two-tailed, unpaired Student's t-test (***$p < 0.001$) of three different experiments.

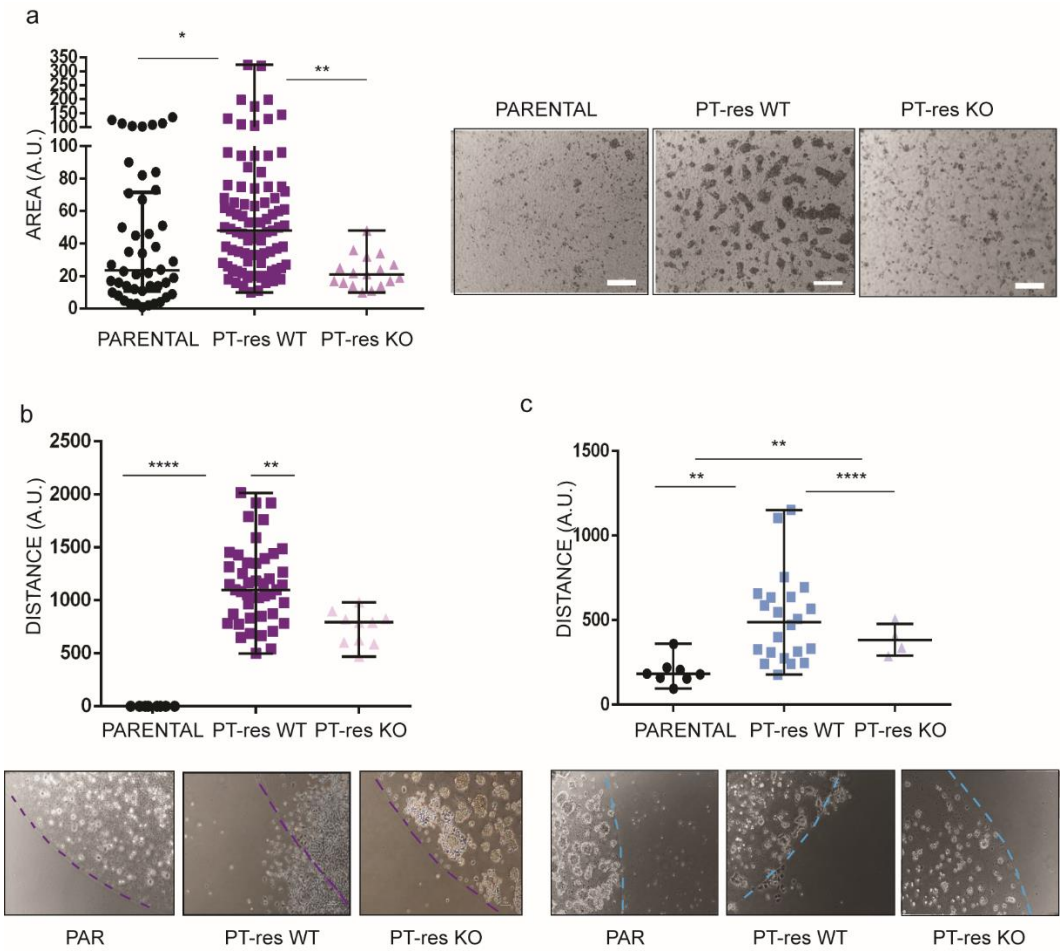

Figure 11: Growth on mesothelial cells and evasion assay (**a**) TOV-112D Parental, PT-res WT and KO were evaluated for their ability to adhere and growth on a mesothelial cells monolayer. Area of spheroids were evaluated on the left panel. Representative images of the experiment are on the right. (**b**) Matrigel evasion assay of TOV-112D Parental, PT-res WT and ITGA6 KO cells. Graph (top) reports the distance covered by the individual cells from the edge of the drop. Representative phase-contrast images are reported in the bottom panels. (**c**) Matrigel evasion assay of OVSAHO Parental, Pt-res WT and ITGA6 KO cells. Graph reports the distance covered by the individual cells from the edge of the drop. In (**a**) (**b**) and (**c**) statistical significance was determined by a two-tailed, unpaired Student's t-test (***$p < 0.001$) of three different experiments.

4.3 ITGA6 is transcriptional induced by CDDP treatments. The data collected so far demonstrated that ITGA6 is overexpressed in PT-res cells and that its expression mediate, at least in part the resistance to CDDP of these cells possibly by promoting adhesion to ECM and mesothelial cells and/or by sustaining the acquisition of a CSC-like phenotypes**.**

By quantitative Real-Time PCR analysis, we observed that ITGA6 mRNA was tenfold more expressed in PT-res clones than the Parental counterpart of both TOV-112D and OVSAHO (Figure 6a), suggesting that its overexpression was due to transcriptional regulation.

Since PT-res cells were selected by progressive CDDP treatments, we wondered if CDDP could induce ITGA6 transcription that then remain highly expressed in a resistant tumour subpopulation. To answer this question, we first used time course mRNA analysis of parental cells treated with

CDDP 25μM at short time point showed that ITGA6 mRNA level significantly increased in a time-dependent manner in both cell lines (Figure 6b) suggesting that ITGA6 transcription is activated by CDDP to possibly contribute to PT-resistance.

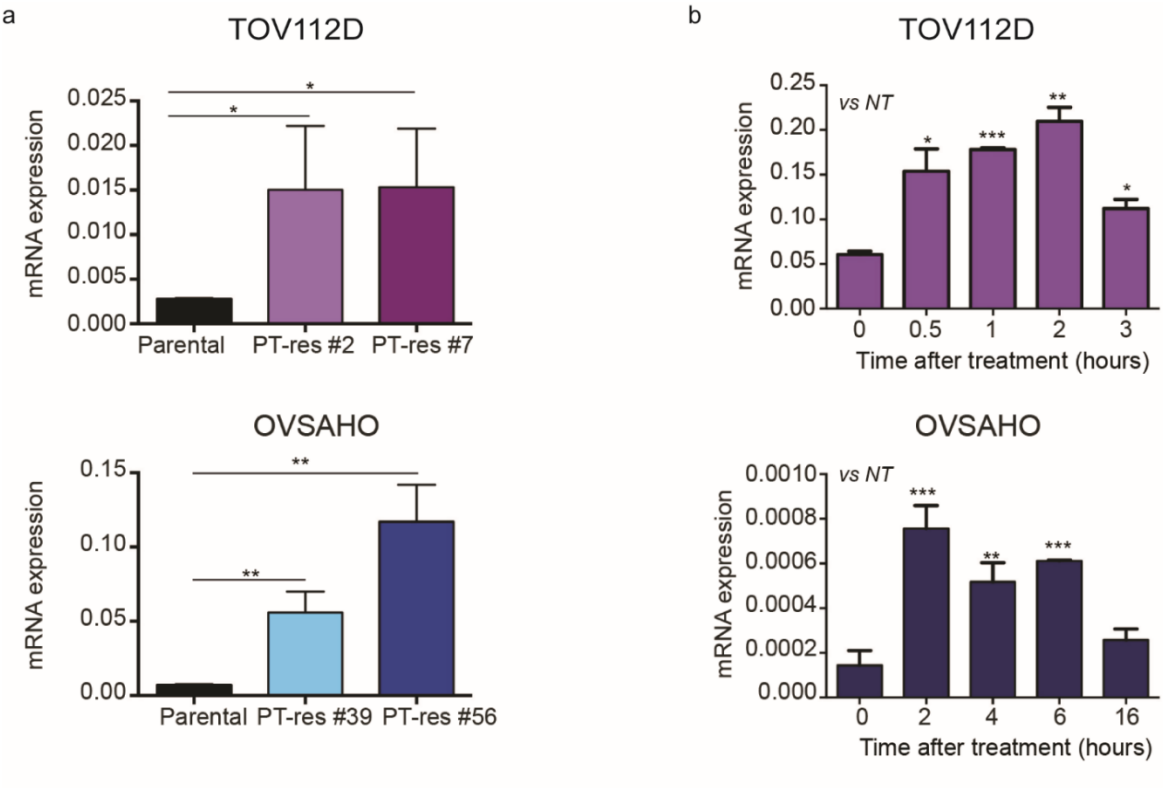

Figure 6 ITGA6 is transcriptionally induced by CDDP: (**a**) Expression of ITGA6 in parental and PT-res cells in both TOV-112D and OVSAHO. **(b)** Expression of ITGA6 in both TOV-112D and OVSAHO parental cells was evaluated in treatment with cisplatin (CDDP) (25μM) at the indicated time. In **(a)** and **(b)** mRNA levels was evaluated by RT-qPCR analyses, in triplicate and normalized using ACTIN housekeeping gene. Data represent the mean ± SD of 3 biological replicates, performed in duplicate. Statistical significance was determined by a two-tailed, unpaired Student's t-test (ns = Not Significant, *p < 0.05, **p < 0.01, ***p < 0.001).

To investigate more in detail the molecular mechanism by which ITGA6 transcription was activated by CDDP, we cloned the promoter region of ITGA6 into the pGL3-Luc reporter vector. Luciferase reporter assay in TOV-112D parental cells demonstrated that CDDP increased of about 4 folds the activity of ITGA6 promoter (Figure 7a and b).

Two putative transcription factors for ITGA6 transcription that are mostly deregulated in cancer models: c-MYC and SP1 [78] (Figure 7a). To understand if one or both transcription factors were involved in the regulation of ITGA6 by CDDP we co-transfected the Luc reporter vector in TOV-112D Parental together with c-MYC or SP1 expressing vectors. Luciferase assay showed a two-fold increase in ITGA6 promoter activity by SP1 overexpression, while the reporter activity was significantly reduced after c-MYC overexpression (Figure 7c). The treatment with Mythramycin (MTA, an SP1 inhibitor) or 10058-F4 (c-MYC-MAX inhibitor) confirmed the data obtained with

genes overexpression showing that ITGA6 promoter activity was significantly reduced after SP1 inhibition and, conversely, upregulated by c-MYC impairment (Figure 7c). These data suggested that the transcription factor involved in the ITGA6 transcriptional activation in our cell models could be SP1. Accordingly, western blot analysis on lysates of TOV-112D overexpressed for Sp1 or treated with MTA for different time points showed that Sp1 overexpression induced a strong increase in ITGA6 protein levels (Figure 7d), while MTA treatments a strong decrease in a time-dependent manner (Figure 7e). Finally, chromatin immunoprecipitation (ChIP) assay followed by qRT-PCR in TOV-112D Parental e PT-res cells treated or not with CDDP showed that, both in Parental and in PT-res cells, SP1 but not c-MYC was enriched at the ITGA6 promoter. More importantly, this enrichment was increased under CDDP pressure only in PT-sensitive cells (Figure 7f), supporting the possibility that SP1-mediated ITGA6 transcription is activated by CDDP as an escaping mechanism adopted by PT-sensitive cells to survive the pressure of PT.

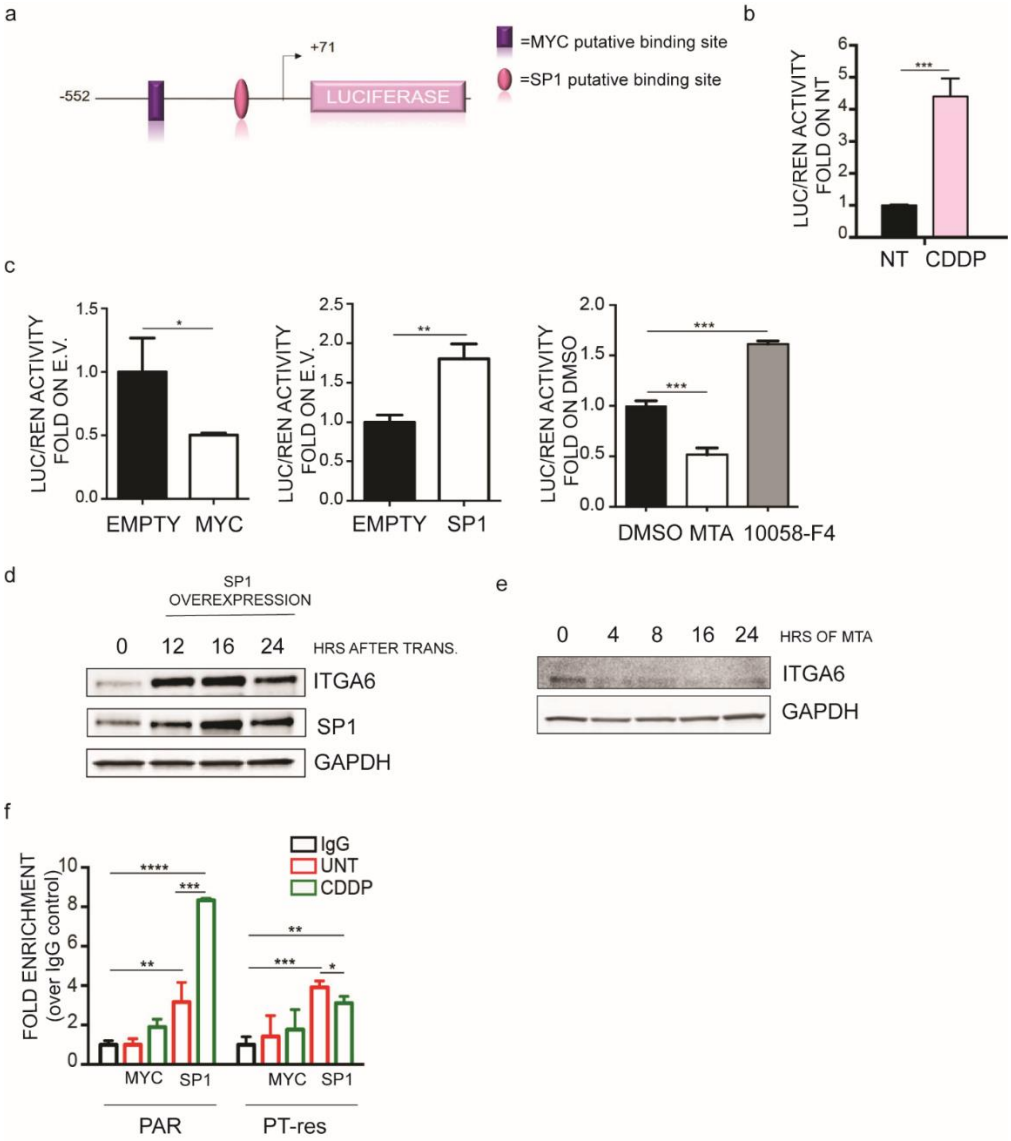

Figure 7: SP1 modulates ITGA6 expression: **(a**) Schematic design of the pGL3-vector used to test the potential c-MYC and SP1 binding sites in the ITGA6 promoter region. Vector is measured based on the distance from ITGA6 transcription start site. (**b**) Graph reporting the normalized Luciferase activity of ITGA6 Full-length promoter fragment in TOV-112D cells treated, after 48h from transfection, with CDDP (25μM) for 24h. (**c**) Graph reporting the normalized Luciferase activity of ITGA6 promoter fragments in TOV-112D cells transfected with c-MYC or SP1 vector or TOV-112D were treated, 48h after transfection, with Mithramycin (MTA) (1μM) and 10058-F4 (1μM) for 24h (**d**)Western blot analysis of the SP1 transcription factors and the ITGA6 in TOV-112D parental cells after transfection at the indicated time. (**e**) Western blot analysis ITGA6 in TOV-112D and OVSAHO parental cells during MTA treatments (1μM) at the indicated times. GAPDH was used as loading control. (**f**) Chromatin immunoprecipitation (ChIP)

4.4 ITGA6 isoforms are regulated by CDDP and c-MYC. ITGA6 can be subjected to alternative splicing at the post-transcriptional level, giving rise to different isoforms (ITGA6A and ITGA6B) which diverge in the cytoplasmic domain[79]. It has been demonstrated that ITGA6B variant, in contrast with the variant ITGA6A, is more linked to the establishment of a stem-like mesenchymal phenotype in breast cancer [63]. Thus, we checked the levels of ITGA6 alternative isoforms in our PT-res models. qRT-PCR analysis revealed that the mRNA of ITGA6B isoform was higher in both TOV-112D (Figure 8a left) and OVSAHO PT-res cells than the respective Parental ones (Figure 8a right). Moreover, CDDP treatment of TOV-112D cells induced an upregulation of ITGA6B, but not of ITGA6A, mRNA expression in a time-dependent manner (Figure 8a). ITGA6 alternative isoforms are regulated especially by two splicing factors namely Epithelial Splicing Regulatory Protein 1 (ESRP1) and 2 (ESRP2) [52]. These splicing factors are more abundant when cells present an epithelial phenotype producing a shift in ITGA6A isoform. Conversely, when ESRP1 and 2 are expressed at lower levels, there is a shift toward the expression of the ITGA6B isoform. Indeed, qRT-PCR analyses demonstrated that both ESRP1 and ESRP2 are less expressed in PT-res models, in line with the increased ITGA6B expression and the mesenchymal phenotype of these cells (Figure 8c). Intriguingly, it has been reported that c-MYC activation positively correlates with ESRPs upregulation[49]. To verify if c-MYC was involved in the regulation of ESRP1 and 2 also in EOC cells, we treated TOV-112D and OVSAHO cells with the 10058-F4 inhibitor and evaluated the mRNA expression of ESRPs and ITGA6 isoforms by qRT-PCR. As shown in Figure 8d and e, ESRPs levels strongly decrease during c-MYC-inhibitor treatment in both TOV-112D (left panel) and OVSAHO Parental cells (right panel). At the same time points, we observed a significant increase in ITGA6B, but not in ITGA6A, expression levels (Figure 8f). Conversely, c-MYC overexpression (Figure 9a) induced a transcriptional reduction of ITGA6B and a significant increase in ESRPs mRNA expression (Figure 9b and 9c), suggesting that c-MYC activity has a role in the regulation of ITGA6 alternative splicing balance.

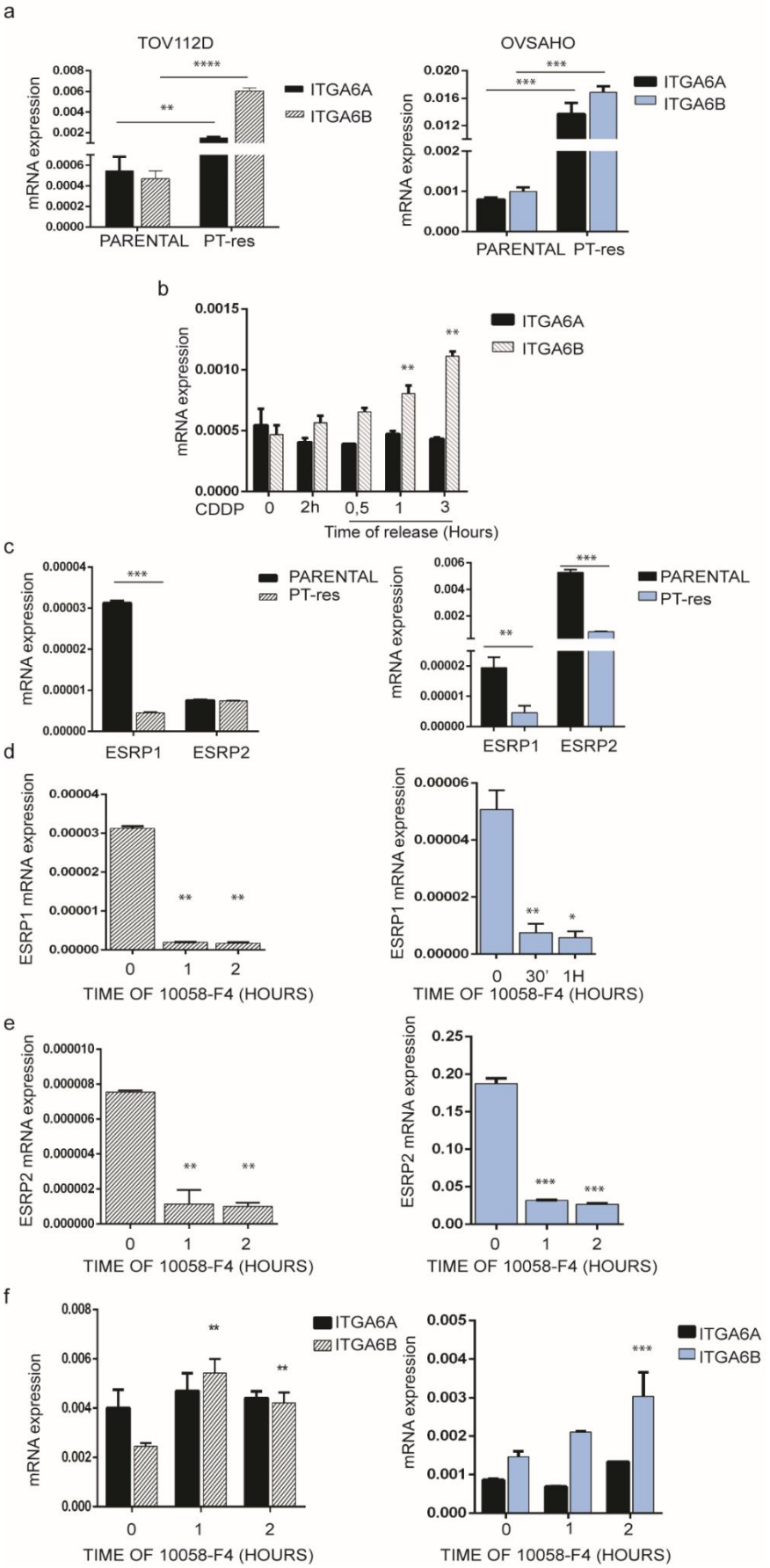

Figure 8 ITGA6 isoforms regulation: ITGA6 trascriptional regulation (**a**) ITGA6 isoforms expression were evaluated in parental and PT-res cells (**b**) Expression of isoforms ITGA6A and ITGA6B was evaluated during and after treatment with CDDP (25μM) at the indicated time points. (**c**) mRNA expression of ESRP1 and ESRP2 were evaluated for Parental and PT-res (**d** and **e**)ESRP1 and ESRP2 expression were evaluated after treatment with c-MYC-MAX inhibitor (10058-F4) at the indicated time points. (**f**) ITGA6 isoforms expression were evaluated in parental cells after treatment with c-MYC-MAX inhibitor (10058-F4) ant the indicated time point. (**c, d, e and f**) mRNA expression were evaluated in both TOV-112D (left) and OVSAHO (right) cells.

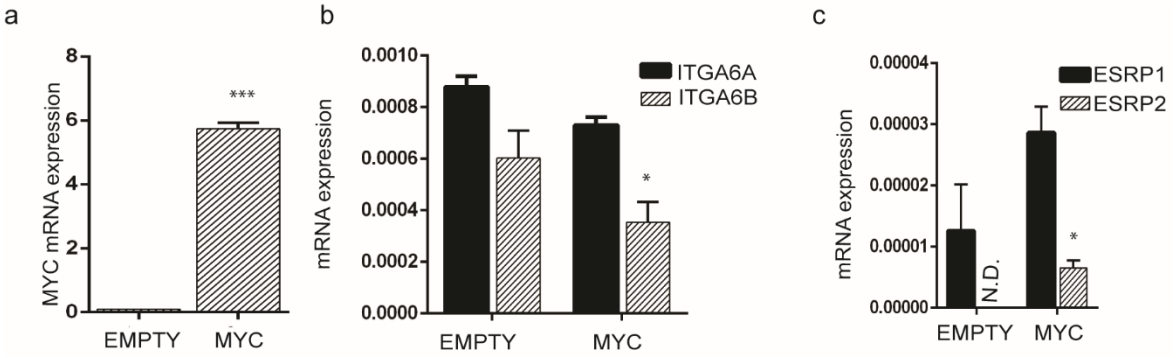

Figure 9 c-MYC modulates ITGA6 isoforms: (**a**) Overexpression of c-MYC in TOV-112D parental cells was verified 16h after transfection with MYC vector. (**b**) ITGA6 mRNA isoforms expression were evaluated after c-MYC overexpression. (**c**) ESRP1 and ESRP2 mRNA expression were evaluated after c-MYC overexpression .

4.5 ITGA6 effects on tumour microenvironment: spheroids adhesion on mesothelial cells

Since we observed a transcriptional increase in ITGA6 during CDDP treatment in Parental cells (Results 4.3 Figure 6) we wonder whether it paralleled an equal increase in ITGA6 protein. Quite surprisingly, western blot analysis conducted on cells treated with CDDP for up to 24 hours showed no increase in ITGA6 levels (Figure 10a). Moreover, using cycloheximide (CHX) treatment we noticed that ITGA6 protein had similar stability in parental and PT-Res cells (Figure 10b), suggesting that increased protein degradation was not involved in the regulation of ITGA6 protein expression after CDDP treatment.

Based on the notion that oxidative stress induced by PT treatment could induce extracellular vesicles release by altering cell membranes lipid layer[80], we reasoned that the ITGA6 overproduced under PT treatment could be actively secreted and for this reason did not accumulated into the cells. To explore this possibility, we treated TOV-112D Parental and PT-res WT cells with CDDP for 1, 3, 6 and 16 hours and at these time point collected their conditioned mediums (CM) and cell lysates both analysed by western blot. We observed that ITGA6, especially its glycosylated form, was released in the CM and this secretion increased upon treatments in a time-dependent manner both in Parental and in PT-res cells (Figure 10a). At the same time, also CD63, known marker of extracellular vesicles, was released in the medium and increased upon treatments (Figure 10a), suggesting that in our models CDDP induces the secretion of extracellular vesicles containing ITGA6. Of note, it has been demonstrated that in different tumour models exosomal integrins (α6β4, α6β1 and αvβ5) direct organ-specific colonization by fusing with target cells in a tissue-specific fashion, thereby initiating pre-

metastatic niche formation [81]. Thus, we wondered if the presence of ITGA6 in the CM of PT-res cells could influence the microenvironment toward the establishment of a "metastatic niche" providing structural support, for the spreading, adhesion and survival of tumour cells. To this aim we challenged for 16 hours LPL mesothelial cells with the CM produced by WT or ITGA6KO PT-res cells. After the removal of the CM, we plated on mesothelial layer, TOV-112D Parental cells and we leaved them in co-culture for 10 days (Figure 10b). As reported in Figure 10c, we found that Parental cells challenged with the CM of PT-res WT cells forms bigger spheroids, more anchored on mesothelial monolayer, respect to the cells conditioned with the CM of ITGA6KO PT-res cells, that conversely, forms spheroids more similar to the ones formed on not conditioned LPL cells (Figure 10c). These results suggested that ITGA6 secreted by PT-res cells is able to prime mesothelial cells to create a pro-metastatic niche that favoured the adhesion and growth of parental EOC cells. We next tested if ITGA6 secreted by PT-res cells could also prime Parental cells to adhere on the mesothelium and metastasize, as demonstrated for colorectal cancer cells metastasizing to the lung[81]. To test this hypothesis we treated TOV-112D parental cells with the CM of WT and ITGA6KO PT-res cells and then challenged them for their ability to adhere on the mesothelial monolayer or to form spheroids formation on poly-hema plates (Figure 11a). Parental cells conditioned with the CM of PT-res WT cells, form bigger spheroids either on poly-hema (Figure 11c) or on mesothelial cells (Figure 11b), respect to the parental cells untreated or conditioned with the CM from ITGA6 KO PT-res cells. Altogether, these experiments indicated that PT-res cells, by secreting ITGA6 could modify the local microenvironment acting on both mesothelial cells (Figure 10) and on sensitive tumour sub-population(s) (Figure 11), creating a pro-metastatic niche in which EOC cells could more easily grow.

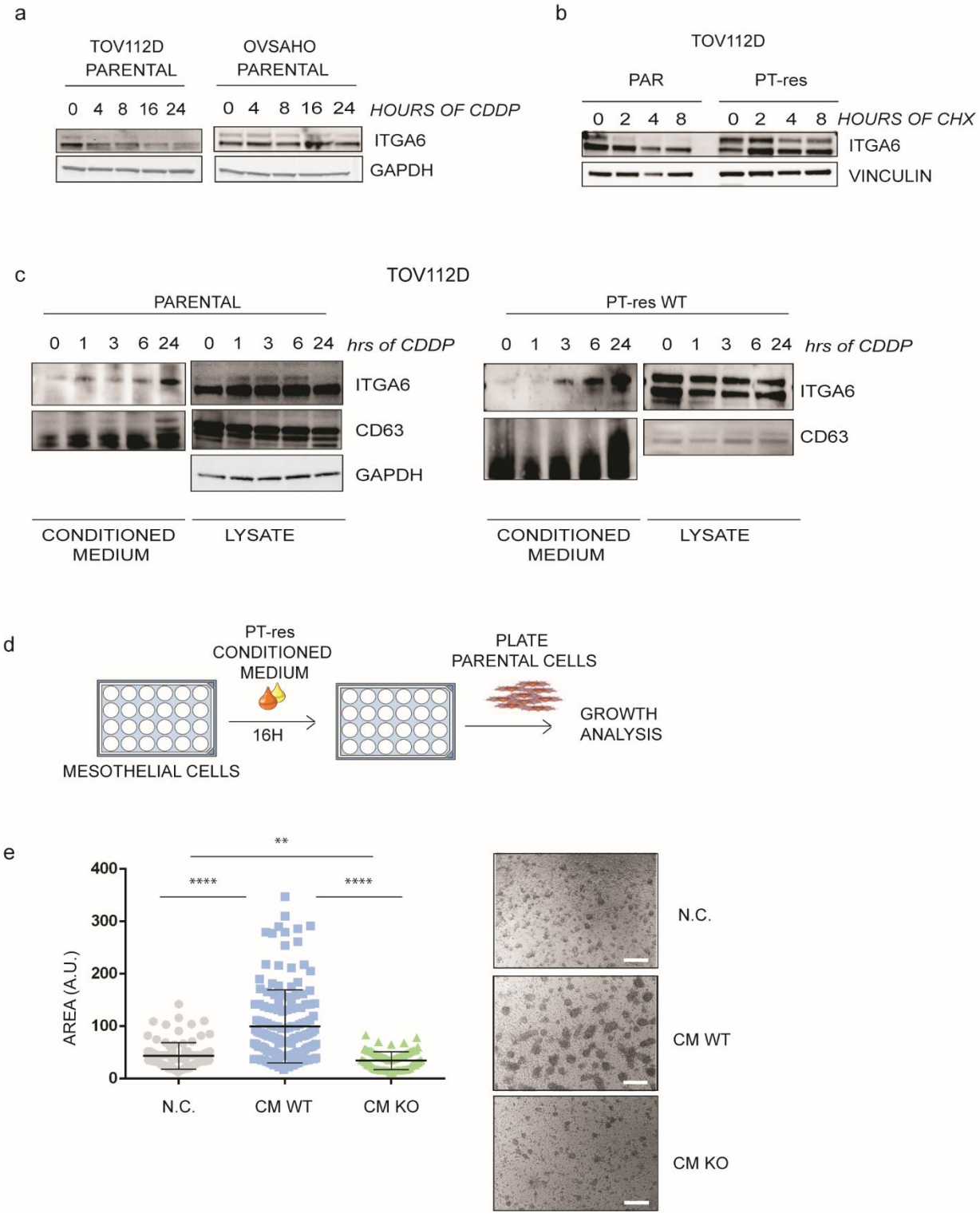

Figure 10: ITGA6 is released in the medium and influence the growth on mesothelial cells.(**a**)Western Blot (WB) analysis of ITGA6 expression level during CDDP treatment at different time point in whole lysates of TOV-112D and OVSAHO Parental. (**b**) ITGA6 protein stability were evaluated after CHX treatments at different time point. For a and b GAPDH and VINCULIN were used as loading control.(**c**) WB analyses of CM (on the left) from TOV-112D Parental and PT-res cells treated or not with CDDP (20µM) evaluating the expression of ITGA6 and CD63 at the indicated time point. The lower panels show the Ponceau staining of the nitrocellulose membranes to check the levels of protein input. *(**d**)* Schematic representation of the experiment procedure. (**e**) On the left, graph reporting the area evaluation of TOV-112D Parental spheres, on mesothelial cells that are pre-exposed or not to CM of PT-res WT or KO. On the right, respresentative images of the experiment. Data represent the mean ± SD of 2 biological replicates, performed in triplicate. Statistical significance was determined by a two-tailed, unpaired Student's t-test (ns = Not Significant, *p < 0.05, **p < 0.01, ***p < 0.001).

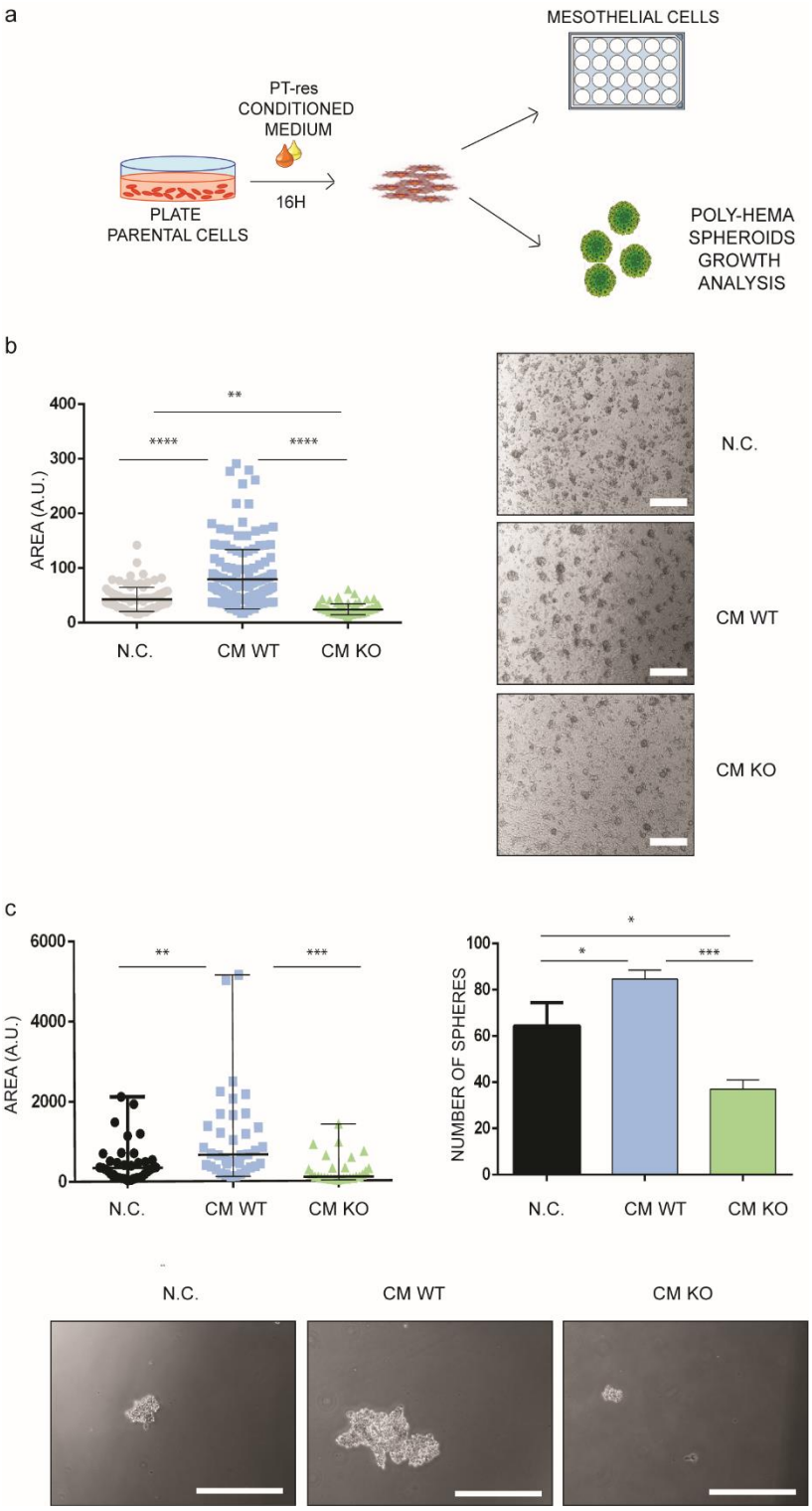

Figure 11 ITGA6 influence TOV-112D spheroids growth and formation: (**a**) Schematic representation of the following experiment. (**b**) On the left, graph reporting the area of TOV-112D Parental spheres, on mesothelial cells. On the right, representative images of the experiment (**c**) Graphs reporting the area and the number of spheroids growth on poly-hema (on the top) and representative images of the experiment on the bottom. For **b** and **c** Parental cells were pre-expose or not for 16h to CM of PT-res WT or KO. Data represent the mean ± SD of 2 biological replicates, performed in triplicate. Statistical significance was determined by a two-tailed, unpaired Student's t-test (ns = Not Significant, *p < 0.05, **p < 0.01, ***p < 0.001).

4.6 ITGA6 drives the increase of EMT markers during adhesion on LM10. Experiments performed so far suggested that PT-res cells expressing high levels of ITGA6, not only facilitates CSC formation and adhesion to the mesothelial cells but also potentially transmits to other cancer cells self-renewal signals through specific intracellular pathways. In this regard, it is well known that stemness and the Epithelial-Mesenchymal Transition (EMT) pathways are molecularly linked and together support metastatic dissemination (as described in introduction). Thus, to investigate in our PT-res models if some of the key regulators of the EMT pathway could be differently regulated after cell adhesion, we cultured TOV-112D PT-res cells either on plastic or on LM10 coated dishes in the presence or not of the anti ITGA6 blocking antibody GoH3. Whole cell lysates were then analysed by western blot. After 1-hour of adhesion of PT-res cells on LM10, we appreciated an upregulation of SNAIL, SLUG and TWIST expression level respect to plastic-adhesion condition (Figure 13a)

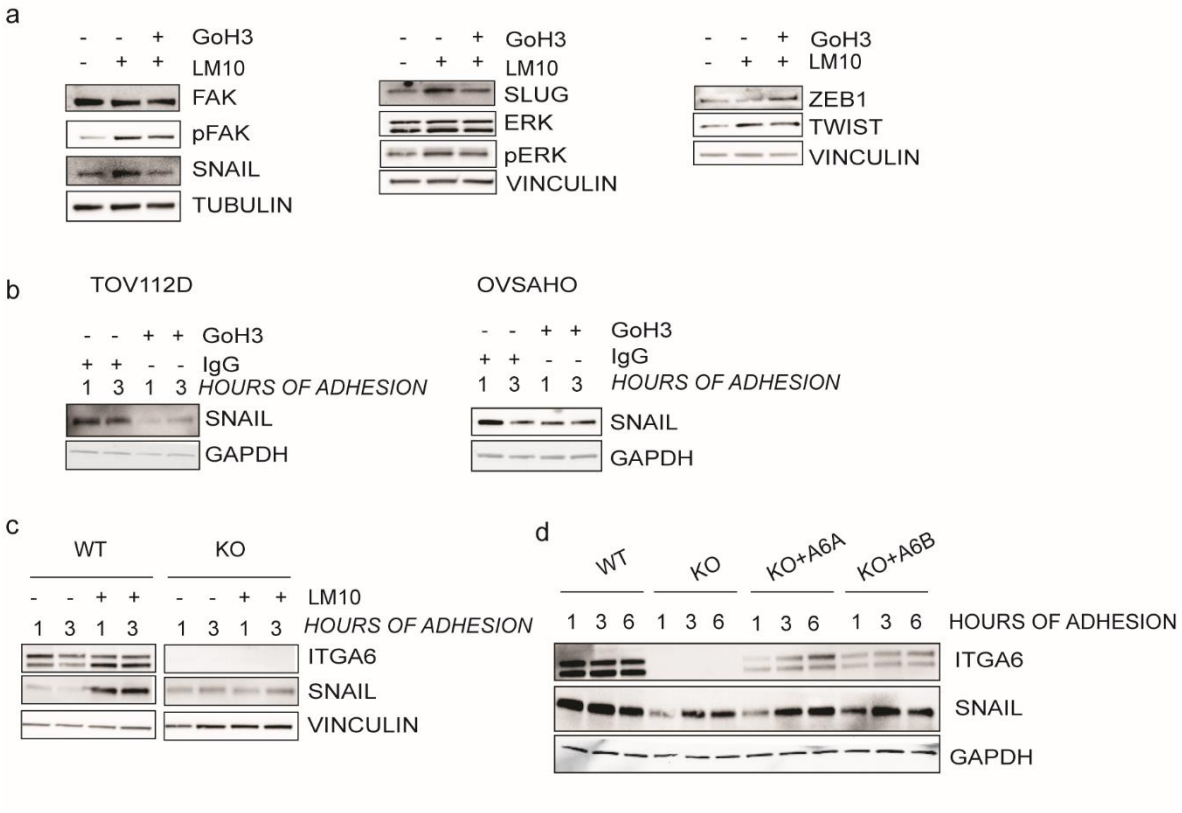

Figure 12: **SNAIL is regulated by ITGA6 during adhesion on LM10** (**a**) Western blot (WB) analysis of TOV-112D PT-res WT after 1h adhesion in plastic, LM10 plus IgG or LM10 plus GoH3. Different protein were evaluated FAK, SNAIL, SLUG, TWIST, ZEB1 and ERK. (**b**) WB analysis of SNAIL protein level after 1 or 3 hours of adhesion on LM10 with IgG or GoH3 was evaluated in both TOV-112D and OVSAHO. (**c**) SNAIL protein level was verified after 1 or 3 hours of adhesion +/- LM10 in TOV-112D PT-res WT or KO. ((**f**) WB analysis of SNAIL expression in TOV-112D PT-res WT, KO and KO transiently overexpressed ITGA6A or ITGA6B. GAPDH, TUBULIN and VINCULIN are used in **a**, **b**, **c**, **d**, **e** and **f** as a loading control

The inhibition of ITGA6-mediated signalling by the GoH3 treatment affected only the upregulation of SNAIL and SLUG, but not of TWIST, suggesting that after adhesion on LM10 these two proteins

were in some way boosted by the activity of ITGA6. We then confirmed that GoH3 treatment affected SNAIL expression in both TOV-112D and OVSAHO PT-res cells during adhesion on LM10 in a time-dependent manner (Figure 13b). To confirm the results obtained with GoH3 blocking antibody, we assessed the SNAIL protein expression in cell lysates of TOV-112D PT-res WT and ITGA6KO cells after 1 and 3 hours of adhesion on either plastic or on LM10 coated dishes. As expected, the absence of ITGA6 significantly abrogated the LM-mediated increase of SNAIL expression that was evident only for PT-res WT cells (Figure 13c). Moreover, re-expression of both isoforms ITGA6A and ITGA6B rescued the upregulation of SNAIL level after 1, 3 and 6 hours of adhesion on LM10 in PT-res KO cells (Figure 13e), confirming that activation of ITGA6 after LM10 adhesion can regulate SNAIL overexpression.

To clarify how ITGA6 could control SNAIL expression after cell adhesion, we first performed qRT-PCR analysis of SNAIL mRNA after 3 hours of adhesion on LM10 or on poly-lysine of PT-res WT and ITGA6KO cells. Figure 14a showed that SNAIL mRNA levels did not increase after laminin adhesion and, more importantly, no difference in its expression were evident between PT-res WT and KO, excluding that ITGA6-derived signalling could regulate SNAIL transcription. SNAIL is a very labile protein with short half-life, actively degraded by proteasome[82]. Therefore, we first checked SNAIL protein level in PT-res WT and ITGA6KO cells plated on LM10 and treated with the proteasome inhibitor MG132. After 1 and 3 hours of adhesion, MG132 induced similar accumulation of SNAIL protein in both PT-res WT and ITGA6KO TOV-112D and OVSAHO cells (Figure 14b), supporting the possibility that the lower levels of SNAIL observed in ITGA6 KO cells were due to more active protein degradation. One of the main regulator of SNAIL protein stability is Glycogen synthase kinase 3 beta (GSK-3β) that binds to and phosphorylates SNAIL at two consensus motifs to induce its translocation to the cytoplasm and subsequent degradation[81]. Thus, we checked whether GSK-3β activity could regulate SNAIL stability in our cells by plating Pt-res ITGA6 KO cells on LM10 and then treated them with MG132 or lithium chloride (LiCl), a known GSK-3β inhibitor. As reported in Figure 14c, MG132 treatment increased SNAIL protein levels while GSK-3β inhibition by LiCl, confirmed by its Ser9 phosphorylation, was not associated to SNAIL increased expression (Figure 14b). These data suggested that GSK-3β was not primarily involved in SNAIL protein stability due to ITGA6-mediated adhesion.

To get a more comprehensive idea about the molecular pathways activated by ITGA6 to regulate SNAIL stability, we used a phospho-antibody array and assessed the phosphorylation of 71 receptor tyrosine kinases (RTKs) in PT-res WT and KO cells allowed to adhere on LM10. Only few RTKs were phosphorylated in these experimental conditions in both cell lines namely the Receptor tyrosine kinase-like orphan receptor 1 (ROR1), the Focal adhesion kinase 1 (FAK) and the Lck/Yes novel

tyrosine kinase (Lyn). Only FAK and Lyn kinases were less phosphorylated in PT-res WT respect to KO cells (Figure 13d). These data were in line with the notion that in acute lymphoblastic leukemia (ALL) cells, ITGA6 depletion lead to an increase of Lyn pY508 and FYN pY530 phosphorylation[83]. More interestingly, other data suggest that Lyn kinase could regulate SNAIL and SLUG protein stability[84]. Thus, we focused further on Lyn kinase activation. Lyn, belongs to the Src-family tyrosine kinases, predominantly expressed in B cells[85]. As for other Src family kinases, Lyn is regulated by protein interactions through its SH2/SH3 domains as well as via phosphorylation status[86]. Phosphorylation on its Tyr 508 residue (Y508) by C-terminal Src kinase (Csk), generates a stabilized inactive kinase confirmation[86]. Conversely, dephosphorylation of the Y508 residue by phosphatases, such as CD45, releases the auto-inhibitory configuration of the kinase domain leading the trans-self-phosphorylation on Tyr397 (Y397) to generate a highly active enzyme[87]. Therefore, we first verified Lyn phosphorylation status in our PT-res WT and ITGA6KO cells and we found that, while phosphorylation on Y397 was non detectable in both WT and ITGA6KO PT-res cells, the inhibitory phosphorylation at Y508 was increased in PT-res KO, confirming the array data and suggesting an involvement of ITGA6/Lyn axis in our cell models (Figure 13e). Further experiments are in progress to verify if in PT-Res cells ITGA6-mediated adhesion regulates SNAIL stability acting on Lyn phosphorylation.

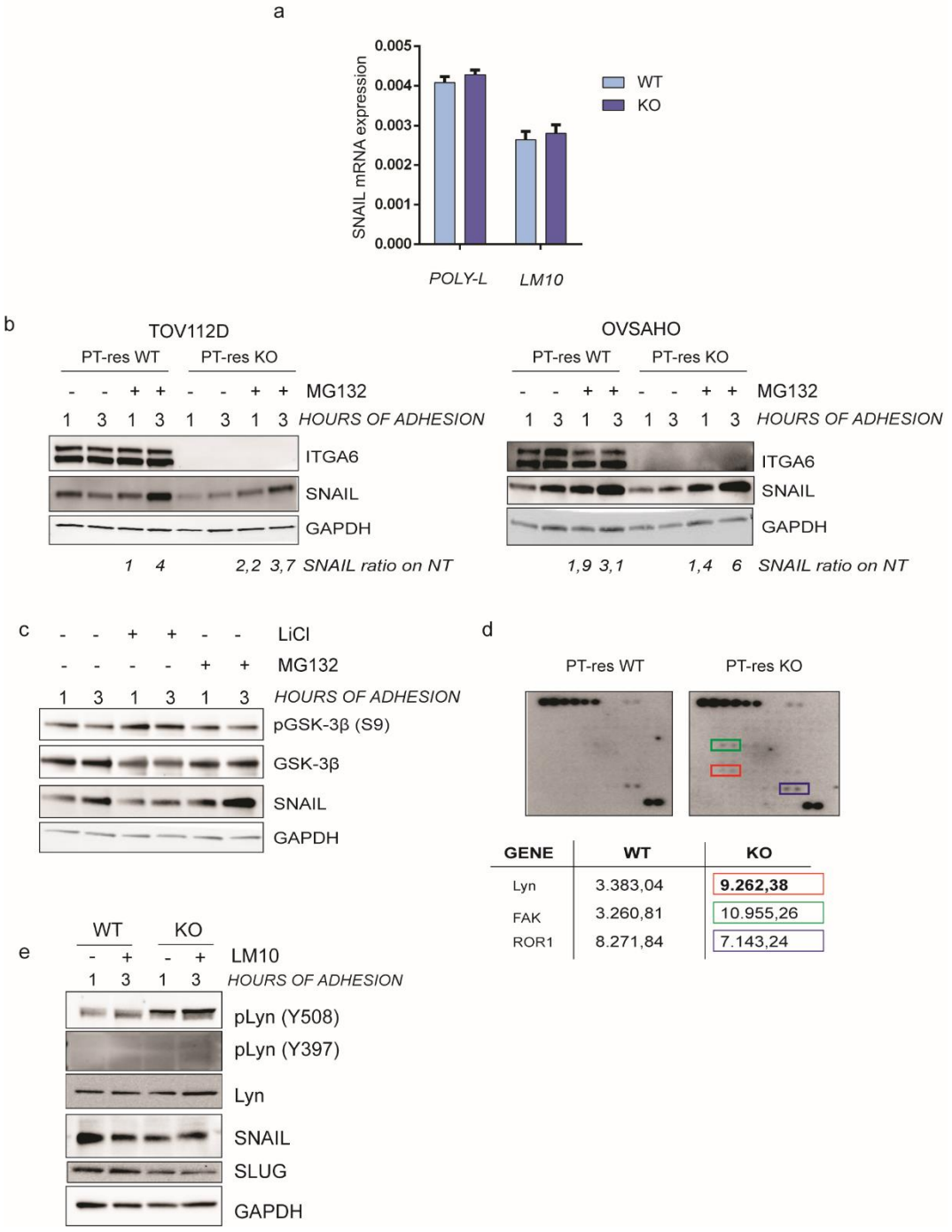

Figure 13: **SNAIL regulation upon adhesion, and RTKs array** (**a**)Expression of SNAIL in PT-res WT and KO were evaluated after 3h of adhesion on poly-lisine or on LM10. Statistical significance was determined by a two-tailed, unpaired Student's t-test (***$p < 0.001$). (**b** and **c**) SNAIL protein level was evaluated by WB after 1 or 3 hours of adhesion on LM10, in TOV-112D and OVSAHO PT-res WT or KO, with or without MG132 (10uM) or lithium chloride (1 mM). GAPDH was used as loading control. (**d**) Protein arrays showing RTKs expressed by TOV-112D PT-res WT (left) and KO (right); boxed spots highlight differentially expressed cytokines. On the bottom table reports quantification expressed in arbitrary units of the protein spots of the experiments: red, green and blue boxes correspond to Lyn, Fak and Ror1 quantification respectively. (**e**) LYN phosphorylations are evaluated by WB after 1 or 3 hours of adhesion on LM10, in TOV-112D PT-res WT or KO. SNAIL and SLUG are evaluated also. GAPDH was used as loading control.

4.7 ITGA6 is necessary for metastatic dissemination of PT-res cells in mouse models.

Having collected several *in vitro* evidences demonstrating that ITGA6 is a key mediator of PT-res cells ability to adhere and growth on mesothelial cells, we asked whether we could translate these *in vitro* observations into *in vivo* evidences. To this aim we intraperitoneally (i.p.) injected TOV-112D PT-res WT and ITGA6KO cells in female NSG mice and assessed tumour spreading both by examination at necroscopy and by pathological analyses. Evaluation of tumour growth showed that the number of i.p. masses developed in mice injected with WT cells was significantly higher than the ones found in mice injected with ITGA6KO cells (Figure 14a). Combined macroscopic and pathological analyses revealed that PT-res WT cells disseminated more efficiently into the peritoneal cavity (particularly liver, pancreas and omentum, which are the typical sites of metastasis encountered in women with advanced stage EOC), while PT-res ITGA6KO cells only marginally engrafted the abdominal organs (Figure 14b-d). Moreover, only in mice injected with PT-res WT cells consistently developed malignant ascites (n= 4/5 for WT and 1/5 for ITGA6 KO injected mice). Finally, the analyses of protein lysates from tumour masses formed by PT-res WT and ITGA6KO cells demonstrated that SNAIL was significantly less expressed in tumour masses formed by ITGA6KO cells compared to tumours formed WT cells (Figure 14e), confirming *in vivo* what observed *in vitro*. Altogether, these data confirmed that ITGA6 plays a crucial role in PT-res cells growth and spreading *in vivo* in mice.

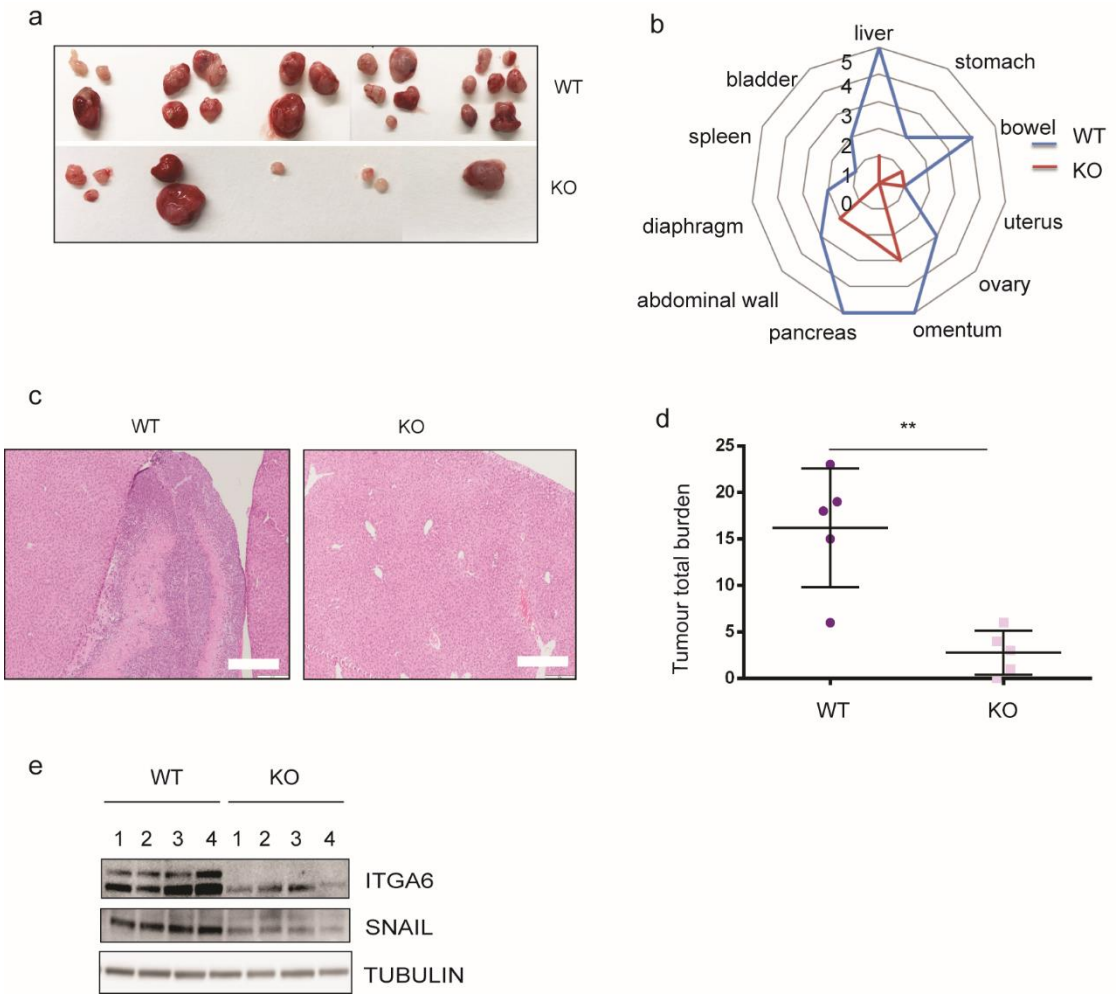

Figure 14 In vivo experiments: (**a**) Tumours images collected from mice injected with PT-res WT (upper part) and PT-res KO (bottom part). Dot (**d**) and radar (**b**) plots reporting the total number of organs colonized and the distribution of abdominal metastasis (**b**) in mice injected intraperitoneally with TOV-112D PT-res WT and ITGA6 KO as determined by macroscopic and pathological analyses. (**c**) Typical images of hematoxylin and eosin (H&E) analyses of the liver area, where the bulk tumor masses were localized in mice injected with WT cells (right). (**e**) SNAIL and ITGA6 protein expression were evaluated in mice tumour masses. TUBULIN is used as loading control.

4.8 Role of ITGA6 in EOC patient's samples.

We next wonder whether what was observed in our model systems could be recapitulated in the human pathology. Taking advantages from a panel of primary EOC cell culture derived from the ascites of PT-Sensitive (n=3) and PT-Resistant (n=5) EOC patients collected in our lab, we evaluated ITGA6 expression by western blot analysis and confirmed that it was upregulated in cells derived from PT-resistant patients (Figure 15a, lane 4-8). Based on the notion that ITGA6 was secreted by EOC cells especially after CDDP treatment (Figure 10), we quantified by ELISA assay the amount of ITGA6 in coupled ascitic samples of 6 EOC patients taken before platinum based-chemo (P=primary) and at tumour relapse or during chemo, (R=relapse). Interestingly, ITGA6 expression increased in 4 out of 6 patients during progression of the disease (Figure 15b). Next, we evaluated the ability of Primary and Relapse ascites samples (from patient 4) to prime LPL mesothelial cells to

tumour growth. To this aim 2% ascites of P and R samples were used to challenge LPL cells for 16 hours in the presence/absence of the GoH3 antibody. Then spheroid formed by TOV-112 cells Parental were allowed to adhere and grow on conditioned LPL cells. Collected data clearly showed that secreted ITGA6 present in the ascites of EOC patients increased the ability of EOC cells to adhere and grow on mesothelial cells (Figure 15c and d).

Finally, based on the above showed data, we postulated that secreted ITGA6 could be also detected in patient's circulation and used as non-invasive prognostic biomarker during/after chemotherapy. Thus, we evaluated ITGA6 expression in a panel of plasma samples collected from stage III-IV EOC patients who underwent chemotherapy in our Institute (Table 1 Methods section). We collected plasma samples at baseline (i.e. before any treatment) and at the end of PT-based chemotherapy and analysed them by western blot. ITGA6 expression increased after chemotherapy in 80% of the patients (17/21), decreased in 4% (1/21) and was unchanged in 14% (3/21) of the patients (Figure 15d). Collectively, these results underline the fact that ITGA6 is secreted in the circulation of PT resistant EOC patients and support the possibility that it could be used as non-invasive biomarkers to identify patients that could benefit from standard PT-based chemotherapy. To this aim analyses coupling expression data with clinic-pathological variables are in progress to evaluate if basal levels of ITGA6 and/or its variation during chemotherapy could predict the response to chemotherapy in EOC patients.

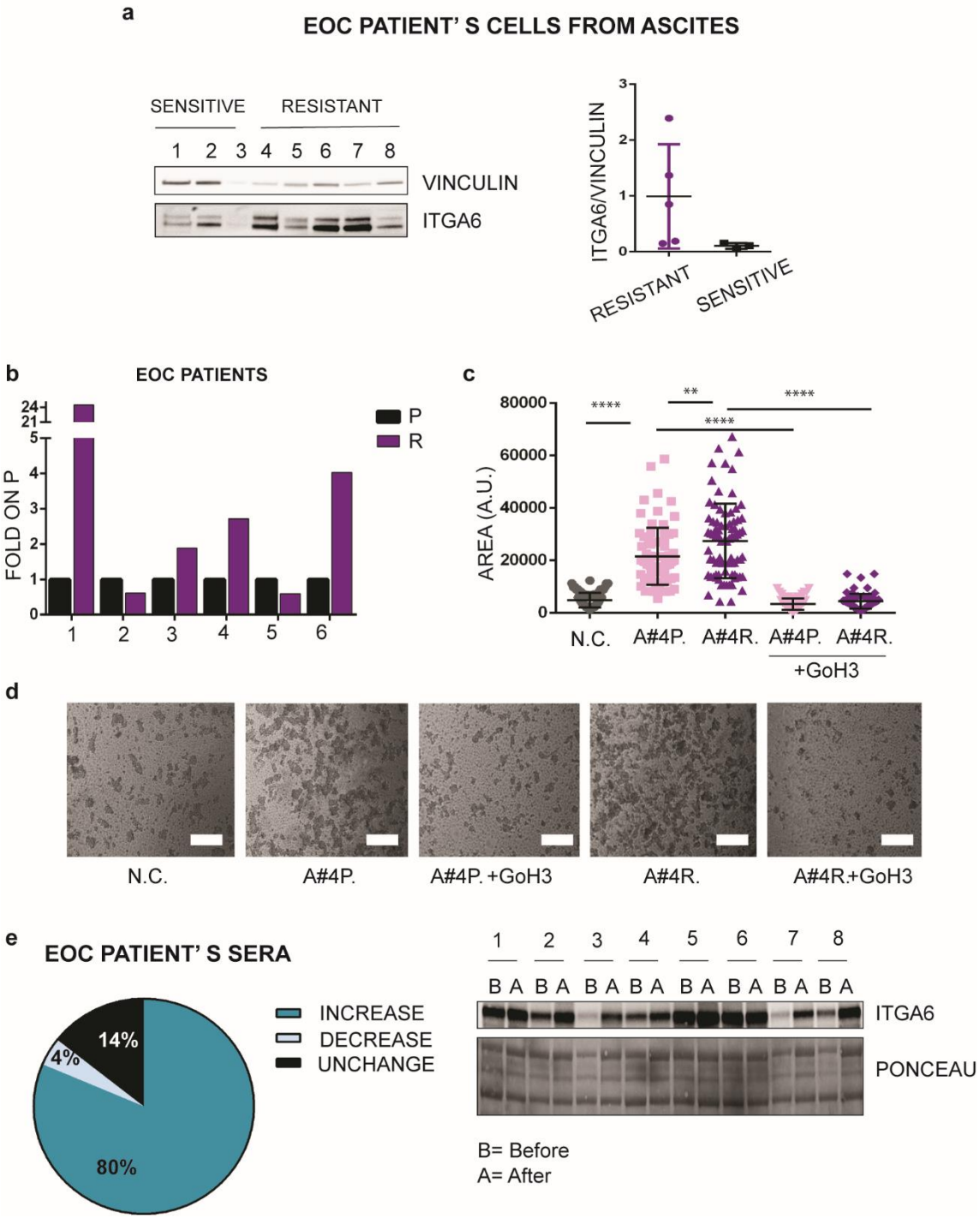

Figure 15 ITGA6 expression in EOC patient's samples: (**a**) ITGA6 expression in primary cells established from EOC ascites samples. The patients were divided in two groups: sensitive and resistant. VINCULIN was used as loading control. (**b**) Graph reporting ELISA analysis comparing ITGA6 expression in patient's ascites during disease progression. For the same patients are represented two columns: the black ones represent the ascites collected before the first-line PT-based therapy; the purple ones represent the ascites collected during progression after chemotherapy (**c**) Graph reporting area of spheroids attached on mesothelial monolayer evaluated with or without challenging with ascites P and R ±GoH3. (**d**) Representative images of the experiment in **d**.(**e**) Representative WB analysis of ITGA6 level in EOC patient's sera collected before (B) and after (A) chemotherapy (on the right). Pie chart summarizing the modification in ITGA6 expression in the plasma samples analysed by WB.

5.DISCUSSION

To date, development of PT-resistance remains the main cause of EOC related death, together with the late diagnosis and the high heterogeneity of the disease. Acquired resistance to chemotherapy has been linked also to microenvironment in which cancer cells can found favourable niche for either CSCs or other tumour cells that are able to repopulate[27]. Moreover, from primary tumour site cancer cells are able to move, in spheroids aggregates and invade other organs[8]. The ascites formation facilitates the dissemination in the peritoneal cavity. In the communication between cells-microenvironment, integrins are the most studied for their unique ability to stimulate inside-out and outside-in signalling. They were described involved in many aggressive phenotype in tumour cells[72]. Here, using an unique panel of isogenic PT-res cells we identified ITGA6 as commonly upregulated in resistant cells and as a key molecule necessary for their adhesion ability on mesothelial cells and on laminin. The fact that ITGA6 functions could be inhibited by a specific blocking Ab suggest that it could represent a druggable target in for PT-resistant EOC. The fact that ITGA6 expression was recently described more expressed in PT-resistant EOC patients by immunohistochemistry analysis[40], and also in PT-resistant EOC PDX [88], reinforce and support our in vitro observation.

Beside mediating cell adhesion and growth on mesothelial cells we also showed that ITGA6 is necessary to sustain the CSCs properties of PT-resistant cells, in line with its expression in several type of stem cells [56]. Indeed, both the use of anti-ITGA6 blocking ab and ITGA6 knock out strongly impaired the ability of PT-res cells to form of ovaryspheres (an accepted surrogate of CSC activity) and their growth on mesothelial cells. It has to be noted that sphere formed from PT-res but not parental cells were insensitive to CDDP treatment. In this context we noticed that ITGA6KO on one side reduce the number and the size of sphere formed by PT-res cells but on the other are not more sensitive to CDDP. These data could either indicate that ITGA6 is expressed by PT-resistant EOC but it is not the cause of drug resistance or could suggest that ITGA6 should be engaged by its ligands (e.g. Laminins) to protect from PT-induced death. This hypothesis is also supported by our data showing that PT-res ITG6KO cells are less resistant to the CDDP treatment than the WT ones especially after adhesion to ECM substrates . One interesting and novel results we report in this thesis is the observation that PT treatment rapidly induced ITGA6 transcription. We deeply investigated how ITGA6 is modulated by PT and verified that it is transcriptionally activated by the engagement of SP1 on its promoter upon CDDP treatment. We still have to define how CDDP favours the binding of SP1 to the ITGA6 promoter acting for instance on SP1 post-translational modification and/or its expression and/or on the general chromatin accessibility. Indeed, recent evidences in lung cancer cells suggest that genes involved in ECM remodelling and cell cycle regulation dominate the process of dormancy and reactivation upon exposure to CDDP and that SP1 is among the most relevant transcription factors regulating their expression via chromatin accessibility of gene promoter. [89].

Future studies are planned to verify if the same is also true in EOC cells and if chromatin accessibility is differently regulated in parental and PT-resistant cells.

On the other hand, we do not identified MYC as a transcription factor able to bind to and regulate ITGA6 promoter. However, we showed that MYC is able to regulate two splicing factors, ESRP1 and 2, eventually influencing the ratio between ITGA6A and ITGA6B isoforms expression. MYC inhibition produces a shift in ITGA6B production, usually associated with a more mesenchymal and aggressive phenotype, and was also the one more transcribed by our PT-res models. Accordingly, PT-res cells express lower level of ESRPs, splicing factors respect to parental cells. This indicates again their transition from an epithelial to mesenchymal phenotype in line with the more aggressive features described in functional experiment.

These data collectively suggest data CDDP treatment in EOC cells rapidly (i.e. within few hours of treatment) induced a transcriptional program that led to the transcription of specific splicing forms of ITGA6. The fact that in this transcriptional program are involved two known oncogenic transcription factors like SP1 and c-MYC both involved in the regulation of EMT suggest that they could participate in the diction of a rapid change of status from epithelial to mesenchymal that is necessary for EOC to metastasize. In fact, it has been proposed that in EOC the EMT program is only partially executed by metastasizing cells that should instead fluctuate from an epithelial and a mesenchymal status, a condition necessary to survive in suspension and rapidly grown upon adhesion to the mesothelium. How this partial EMT [90] is regulated in EOC upon PT treatment is something that should be better defined in future work, but our data support the possibility that MYC and SP1 play a central role in this context.

Another important and previously undescribed aspect we report in this thesis is the fact that PT induced ITGA6 release in the medium. Whether the increased secretion of ITGA6 is the result of a boosted vesicles formation or the consequences of the direct interaction of CDDP with the plasma membrane is something that should be verified in the future. These data are however in agreement with the observation that, in other type of cancers, ITGA6 with its β partners is released in the medium as components of the vesicles membranes driving metastasis in specific organs [81]. In any case our data demonstrated that secreted ITGA6 is active and could cancer cells spreading and growth of the mesothelial monolayer activating a metastasis cascade process. Our data support that PT-res cells are able in this way to not only resist and grow after chemotherapy, but also to commit the microenvironment and other sensitive tumour cells to grow and adhere on mesothelial cells. It was even more interesting the fact that ITGA6 was expressed by PT-resistant cells collected from patients ascites samples and also directly detected in the ascitic fluid where its concentration seems to increase during cancer progression and under chemotherapy treatment.

Overall the picture that come from this thesis work is that the pressure of PT-based chemotherapy on EOC cells drive the activation of a transcriptional program that, among other changes, induced the production of ITGA6. High expression of ITGA6 on one side favours the acquisition of a PT-Resistant phenotype and on the other results in ITGA6 secretion necessary to form a pro-metastatic niche in which EOC cells could more easily adhere and grow.

We also started to explain how ITGA6 derived signalling sustains this program once activated. We showed, in fact, that ITGA6 engagement is necessary to induce the expression of the SNAIL transcription factor family, necessary to prevent their proteasome-mediated degradation. To do this ITGA6 regulate the activity of the Lyn Src-family member kinase that in turn could regulate Snail (and possibly Slug) phosphorylation and expression[84]. We are aware that some passages of this signalling pathway newly described in EOC should be better experimentally proved but we think that the produced evidences are already sufficient to sustain this possibility.

It is worth nothing that our in vitro experiments are strongly supported by in vivo evidences demonstrating that the absence ITGA6 almost completely prevents the growth and metastatization of PT-res cells injected intraperitoneally in NSG mice and strongly impaired the expression of SNAIL in the few grown tumours. Since we largely proved in vitro that the use of an anti-ITGA6 blocking ab like the GoH3 prevent the adhesion of PT-res cells to ECM and mesothelial cells and also block the pro-metastatic effects of conditioned mediums and ascites, we have already planned in vivo experiment to test the efficacy of GoH3 as anti-cancer agent able to block the growth and the metastatic spreading of PT-res EOC. It will also be interesting to test if the usage of GoH3 can block the invasion after the occurrence of ascites and, in the future, design specific clinical trials with clinical grade monoclonal antibodies. Patients at early stage could benefit of the monoclonal therapy in maintenance after standard care, preventing the invasion of those cells that escape chemotherapy. The monoclonal therapy could be an option also for patients at late stage with ascites, preventing the growth an the adhesion of spheroids in the ascites, the monoclonal therapy could decelerate the progression of the disease. Finally, further studies are necessary to better understand the relevance of ITGA6 detected in patients' plasma samples and its potential as prognostic/predictive marker allowing to discriminate EOC patients that could benefit of an anti ITGA6-targeted therapy.

6.REFERENCES

1. Jayson, G. C., Kohn, E. C., Kitchener, H. C. & Ledermann, J. A. Ovarian cancer. *Lancet* **384,** 1376–1388 (2014).

2. Torre, L. A. *et al.* Ovarian cancer statistics, 2018. *CA. Cancer J. Clin.* **68,** 284–296 (2018).

3. Shih, I.-M. & Kurman, R. J. Ovarian tumorigenesis: a proposed model based on morphological and molecular genetic analysis. *Am. J. Pathol.* **164,** 1511–1518 (2004).

4. Vang, R., Shih, I.-M. & Kurman, R. J. Ovarian low-grade and high-grade serous carcinoma: pathogenesis, clinicopathologic and molecular biologic features, and diagnostic problems. *Adv. Anat. Pathol.* **16,** 267–282 (2009).

5. Goff, B. A., Mandel, L. S., Melancon, C. H. & Muntz, H. G. Frequency of symptoms of ovarian cancer in women presenting to primary care clinics. *J. Am. Med. Assoc.* **291,** 2705–2712 (2004).

6. Bankhead, C. R. *et al.* Identifying symptoms of ovarian cancer: A qualitative and quantitative study. *BJOG An Int. J. Obstet. Gynaecol.* **115,** 1008–1014 (2008).

7. Mitra, A. K. Ovarian Cancer Metastasis: A Unique Mechanism of Dissemination. in *Tumor Metastasis* (InTech, 2016). doi:10.5772/64700

8. Yeung, T. L. *et al.* Cellular and molecular processes in ovarian cancer metastasis. A review in the theme: Cell and molecular processes in cancer metastasis. *Am. J. Physiol. - Cell Physiol.* **309,** C444–C456 (2015).

9. Ahmed, N. & Stenvers, K. L. Getting to know ovarian cancer ascites: Opportunities for targeted therapy-based translational research. *Front. Oncol.* **3 SEP,** (2013).

10. Lengyel, E. Ovarian cancer development and metastasis. *American Journal of Pathology* **177,** 1053–1064 (2010).

11. Nakamura, K. *et al.* cancers Role of the Exosome in Ovarian Cancer Progression and Its Potential as a Therapeutic Target. *Cancers (Basel).* **11,** 1147 (2019).

12. Della Pepa, C. *et al.* Ovarian cancer standard of care: are there real alternatives? *Chin. J. Cancer* **34,** 17–27 (2015).

13. Kellogg, E. H. *et al.* Insights into the Distinct Mechanisms of Action of Taxane and Non-Taxane Microtubule Stabilizers from Cryo-EM Structures. *J. Mol. Biol.* **429,** 633–646 (2017).

14. Lambert, H. E. & Berry, R. J. High dose cisplatin compared with high dose cyclophosphamide in the management of advanced epithelial ovarian cancer (FIGO stages III and IV): report from the North Thames Cooperative Group. *Br. Med. J. (Clin. Res. Ed).* **290,** 889–893 (1985).

15. Piccart, M. J. *et al.* Randomized Intergroup Trial of Cisplatin–Paclitaxel Versus Cisplatin–Cyclophosphamide in Women With Advanced Epithelial Ovarian Cancer: Three-Year Results. *JNCI J. Natl. Cancer Inst.* **92,** 699–708 (2000).

16. Pignata, S. *et al.* Carboplatin Plus Paclitaxel Versus Carboplatin Plus Pegylated Liposomal Doxorubicin As First-Line Treatment for Patients With Ovarian Cancer: The MITO-2 Randomized Phase III Trial. *J. Clin. Oncol.* **29,** 3628–3635 (2011).

17. Malyuchenko, N. V, Kotova, E. Y., Kulaeva, O. I., Kirpichnikov, M. P. & Studitskiy, V. M. PARP1 Inhibitors: antitumor drug design. *Acta Naturae* **7,** 27–37 (2015).

18. Ray-Coquard, I. *et al.* Olaparib plus Bevacizumab as First-Line Maintenance in Ovarian Cancer. *N. Engl. J. Med.* **381,** 2416–2428 (2019).

19. Galluzzi, L. *et al.* Molecular mechanisms of cisplatin resistance. *Oncogene* **31,** 1869–1883 (2012).

20. KONKIMALLA, V. B., KAINA, B. & EFFERTH, T. Role of Transporter Genes in Cisplatin Resistance. *In Vivo (Brooklyn).* **22,** 279 LP-283 (2008).

21. Rodrigo, M. A. M. *et al.* Metallothionein-3 promotes cisplatin chemoresistance remodelling in neuroblastoma. *Sci. Rep.* **11,** 5496 (2021).

22. Yun, J. *et al.* Predictive value of the ERCC1 expression for treatment response and survival in advanced gastric cancer patients receiving cisplatin-based first-line chemotherapy. *Cancer Res. Treat.* **42,** 101–106 (2010).

23. Vousden, K. H. & Lane, D. P. p53 in health and disease. *Nat. Rev. Mol. Cell Biol.* **8,** 275–283 (2007).

24. Branch, P., Masson, M., Aquilina, G., Bignami, M. & Karran, P. Spontaneous development of drug resistance: mismatch repair and p53 defects in resistance to cisplatin in human tumor cells. *Oncogene* **19,** 3138–3145 (2000).

25. Michaud, W. A. *et al.* Bcl-2 Blocks Cisplatin-Induced Apoptosis and Predicts Poor Outcome Following Chemoradiation Treatment in Advanced Oropharyngeal Squamous Cell Carcinoma. *Clin. Cancer Res.* **15,** 1645 LP-1654 (2009).

26. Haslehurst, A. *et al.* EMT transcription factors snail and slug directly contribute to cisplatin resistance in ovarian cancer. *BMC Cancer* **12,** 91 (2012).

27. Aguirre-Ghiso, J. A. Models, mechanisms and clinical evidence for cancer dormancy. *Nat. Rev. Cancer* **7,** 834–846 (2007).

28. Correia, A. L. & Bissell, M. J. The tumor microenvironment is a dominant force in multidrug resistance. *Drug Resist. Updat.* **15,** 39–49 (2012).

29. Barkan, D., Green, J. E. & Chambers, A. F. Extracellular matrix: A gatekeeper in the transition from dormancy to metastatic growth. *Eur. J. Cancer* **46,** 1181–1188 (2010).

30. Zhu, L.-C. *et al.* Membranous expressions of Lewis y and CAM-DR-related markers are independent factors of chemotherapy resistance and poor prognosis in epithelial ovarian cancer. *Am. J. Cancer Res.* **5,** 830–843 (2015).

31. Takagi, J., Petre, B. M., Walz, T. & Springer, T. A. Global Conformational Rearrangements in Integrin Extracellular Domains in Outside-In and Inside-Out Signaling. *Cell* **110,** 599–611 (2002).

32. Chen, S.-H. & Chang, J.-Y. New Insights into Mechanisms of Cisplatin Resistance: From Tumor Cell to Microenvironment. *Int. J. Mol. Sci.* **20,** 4136 (2019).

33. Hynes, R. O. & Naba, A. Overview of the matrisome--an inventory of extracellular matrix constituents and functions. *Cold Spring Harb. Perspect. Biol.* **4,** a004903–a004903 (2012).

34. Barczyk, M., Carracedo, S. & Gullberg, D. Integrins. *Cell Tissue Res.* **339,** 269–280 (2010).

35. Heino, J. The collagen family members as cell adhesion proteins. *BioEssays* **29,** 1001–1010 (2007).

36. Johnson, M. S., Lu, N., Denessiouk, K., Heino, J. & Gullberg, D. Integrins during evolution:

Evolutionary trees and model organisms. *Biochim. Biophys. Acta - Biomembr.* **1788,** 779–789 (2009).

37. Calderwood, D. A. *et al.* The Talin Head Domain Binds to Integrin β Subunit Cytoplasmic Tails and Regulates Integrin Activation*. *J. Biol. Chem.* **274,** 28071–28074 (1999).

38. Cai, X., Thinn, A. M. M., Wang, Z., Shan, H. & Zhu, J. The importance of N-glycosylation on β3 integrin ligand binding and conformational regulation. *Sci. Rep.* **7,** 4656 (2017).

39. Arnaout, M. A., Mahalingam, B. & Xiong, J.-P. INTEGRIN STRUCTURE, ALLOSTERY, AND BIDIRECTIONAL SIGNALING. *Annu. Rev. Cell Dev. Biol.* **21,** 381–410 (2005).

40. Wei, L., Yin, F., Chen, C. & Li, L. Expression of integrin α-6 is associated with multi drug resistance and prognosis in ovarian cancer. *Oncol. Lett.* **17,** 3974–3980 (2019).

41. Shimaoka, M. & Springer, T. A. Therapeutic antagonists and conformational regulation of integrin function. *Nature Reviews Drug Discovery* **2,** 703–716 (2003).

42. Hamidi, H. & Ivaska, J. Every step of the way: integrins in cancer progression and metastasis. *Nat. Rev. Cancer* **18,** 1–16 (2018).

43. Burkhalter, R. J., Symowicz, J., Hudson, L. G., Gottardi, C. J. & Stack, M. S. Integrin regulation of beta-catenin signaling in ovarian carcinoma. *J. Biol. Chem.* **286,** 23467–23475 (2011).

44. Seguin, L., Desgrosellier, J. S., Weis, S. M. & Cheresh, D. A. Integrins and cancer: regulators of cancer stemness, metastasis, and drug resistance. *Trends Cell Biol.* **25,** 234–240 (2015).

45. Yan, L. *et al.* Lewis y enhances CAM-DR in ovarian cancer cells by activating the FAK signaling pathway and upregulating Bcl-2/Bcl-XL expression. *Biochimie* **113,** 17–25 (2015).

46. Wei, L., Yin, F., Zhang, W. & Li, L. STROBE-compliant integrin through focal adhesion involve in cancer stem cell and multidrug resistance of ovarian cancer. *Medicine (Baltimore).* **96,** (2017).

47. Wu, C. & Alman, B. A. Side population cells in human cancers. *Cancer Lett.* **268,** 1–9 (2008).

48. Gebhardt, A. *et al.* Myc regulates keratinocyte adhesion and differentiation via complex formation with Miz1. *J. Cell Biol.* **172,** 139–149 (2006).

49. Groulx, J.-F., Boudjadi, S. & Beaulieu, J.-F. MYC Regulates α6 Integrin Subunit Expression and Splicing Under Its Pro-Proliferative ITGA6A Form in Colorectal Cancer Cells. *Cancers (Basel).* **10,** 42 (2018).

50. Gaudreault, M., Vigneault, F., Leclerc, S. & Guérin, S. L. Laminin Reduces Expression of the Human α6 Integrin Subunit Gene by Altering the Level of the Transcription Factors Sp1 and Sp3. *Invest. Ophthalmol. Vis. Sci.* **48,** 3490–3505 (2007).

51. Zhou, Z. *et al.* α6-Integrin alternative splicing: distinct cytoplasmic variants in stem cell fate specification and niche interaction. *Stem Cell Res. Ther.* **9,** 122 (2018).

52. Warzecha, C. C. *et al.* An ESRP-regulated splicing programme is abrogated during the epithelial-mesenchymal transition. *EMBO J.* **29,** 3286–3300 (2010).

53. Leu, S.-J. *et al.* Identification of a Novel Integrin α6β1 Binding Site in the Angiogenic Inducer CCN1 (CYR61). *J. Biol. Chem.* **278,** 33801–33808 (2003).

54. Shaw, L. M., Messier, J. M. & Mercurio, A. M. The activation dependent adhesion of macrophages to laminin involves cytoskeletal anchoring and phosphorylation of the alpha 6 beta 1 integrin. *J. Cell Biol.* **110,** 2167–2174 (1990).

55. Georges-Labouesse, E. *et al.* Absence of integrin α6 leads to epidermolysis bullosa and neonatal death in mice. *Nat. Genet.* **13,** 370–373 (1996).

56. Krebsbach, P. H. & Villa-diaz, L. G. The Role of Integrin a 6 (CD49f) in Stem Cells : More than a Conserved Biomarker. **26,** 1090–1099 (2017).

57. Hynes, R. O. Integrins: A family of cell surface receptors. *Cell* **48,** 549–554 (1987).

58. Taddei, I. *et al.* Beta1 integrin deletion from the basal compartment of the mammary epithelium affects stem cells. *Nat. Cell Biol.* **10,** 716–722 (2008).

59. Welser-Alves, J. V *et al.* Endothelial β4 Integrin Is Predominantly Expressed in Arterioles, Where It Promotes Vascular Remodeling in the Hypoxic Brain. *Arterioscler. Thromb. Vasc. Biol.* **33,** 943–953 (2013).

60. Borradori, L. & Sonnenberg, A. Structure and Function of Hemidesmosomes: More Than Simple Adhesion Complexes. *J. Invest. Dermatol.* **112,** 411–418 (1999).

61. Kariya, Y. & Gu, Y. K. and J. Roles of Laminin-332 and α6β4 Integrin in Tumor Progression. *Mini-Reviews in Medicinal Chemistry* **9,** 1284–1291 (2009).

62. Chung, J., Clifford, J. L., Soung, Y. H. & Gil, H. J. Role of α6β4 Integrin in Cell Motility, Invasion and Metastasis of Mammary Tumors. *Current Protein & Peptide Science* **12,** 23–29 (2011).

63. Goel, H. L. *et al.* Regulated splicing of the α6 integrin cytoplasmic domain determines the fate of breast cancer stem cells. *Cell Rep.* **7,** 747–761 (2014).

64. Dydensborg, A. B. *et al.* Differential expression of the integrins α6Aβ4 and α6Bβ4 along the crypt–villus axis in the human small intestine. *Histochem. Cell Biol.* **131,** 531–536 (2009).

65. El Mourabit, H. *et al.* The PDZ domain of TIP-2/GIPC interacts with the C-terminus of the integrin α5 and α6 subunits. *Matrix Biol.* **21,** 207–214 (2002).

66. Chang, C. *et al.* A laminin 511 matrix is regulated by TAZ and functions as the ligand for the α6Bβ1 integrin to sustain breast cancer stem cells. *Genes Dev.* **29,** 1–6 (2015).

67. Ran, F. A. *et al.* Genome engineering using the CRISPR-Cas9 system. *Nat. Protoc.* **8,** 2281–2308 (2013).

68. Sonego, M. *et al.* Common biological phenotypes characterize the acquisition of platinum-resistance in epithelial ovarian cancer cells. *Sci. Rep.* **7,** 7104 (2017).

69. Spessotto, P. *et al.* Fluorescence-Based Assays for In Vitro Analysis of Cell Adhesion and Migration BT - Extracellular Matrix Protocols: Second Edition. in (eds. Even-Ram, S. & Artym, V.) 221–250 (Humana Press, 2009). doi:10.1007/978-1-59745-413-1_16

70. Dall'Acqua, A. *et al.* CDK6 protects epithelial ovarian cancer from platinum-induced death via FOXO3 regulation. *EMBO Mol. Med.* **9,** 1415–1433 (2017).

71. Lombardi, R. *et al.* HSP90 identified by a proteomic approach as druggable target to reverse platinum resistance in ovarian cancer. *Mol. Oncol.* **15,** 1005–1023 (2021).

72. Aoudjit, F. & Vuori, K. Integrin signaling in cancer cell survival and chemoresistance. *Chemother. Res. Pract.* **2012,** 283181 (2012).

73. Sekiguchi, R. & Yamada, K. M. Basement Membranes in Development and Disease. *Curr. Top. Dev. Biol.* **130,** 143–191 (2018).

74. Pouliot, N. & Kusuma, N. Laminin-511: a multi-functional adhesion protein regulating cell migration, tumor invasion and metastasis. *Cell Adh. Migr.* **7,** 142–149 (2013).

75. Bigoni-Ordóñez, G. D., Czarnowski, D., Parsons, T. & Villa-Diaz*, G. J. M. and L. G. Integrin α6 (CD49f), The Microenvironment and Cancer Stem Cells. *Current Stem Cell Research & Therapy* **14,** 428–436 (2019).

76. Sonego, M. *et al.* USP1 links platinum resistance to cancer cell dissemination by regulating Snail stability. *Sci. Adv.* **5,** eaav3235 (2019).

77. Walker, C. & Mojares, E. *Role of Extracellular Matrix in Development and Cancer Progression*. (2018). doi:10.3390/ijms19103028

78. Zhang, Y. *et al.* Sp1 and c-Myc modulate drug resistance of leukemia stem cells by regulating survivin expression through the ERK-MSK MAPK signaling pathway. *Mol. Cancer* **14,** 56 (2015).

79. HOGERVORST, F., KUIKMAN, I., VAN KESSEL, A. G. & SONNENBERG, A. Molecular cloning of the human α6 integrin subunit: Alternative splicing of α6 mRNA and chromosomal localization of the α6 and β4 genes. *Eur. J. Biochem.* **199,** 425–433 (1991).

80. Ab Razak, N. S., Ab Mutalib, N. S., Mohtar, M. A. & Abu, N. Impact of Chemotherapy on Extracellular Vesicles: Understanding the Chemo-EVs. *Front. Oncol.* **9,** 1113 (2019).

81. Hoshino, A. *et al.* Tumour exosome integrins determine organotropic metastasis. *Nature* **527,** 329–335 (2015).

82. Mishra, P., Senthivinayagam, S., Rana, A. & Rana, B. Glycogen Synthase Kinase-3beta regulates Snail and beta-catenin during gastrin-induced migration of gastric cancer cells. *J. Mol. Signal.* **5,** 9 (2010).

83. Gang, E. J. *et al.* Integrin α6 mediates the drug resistance of acute lymphoblastic B-cell leukemia. *Blood* **136,** 210–223 (2020).

84. Thaper, D. *et al.* Targeting Lyn regulates Snail family shuttling and inhibits metastasis. *Oncogene* **36,** 3964–3975 (2017).

85. Contri, A. *et al.* Chronic lymphocytic leukemia B cells contain anomalous Lyn tyrosine kinase, a putative contribution to defective apoptosis. *J. Clin. Invest.* **115,** 369–378 (2005).

86. Xu, Y., Harder, K. W., Huntington, N. D., Hibbs, M. L. & Tarlinton, D. M. Lyn Tyrosine Kinase: Accentuating the Positive and the Negative. *Immunity* **22,** 9–18 (2005).

87. Katagiri, T. *et al.* CD45 Negatively Regulates Lyn Activity by Dephosphorylating Both Positive and Negative Regulatory Tyrosine Residues in Immature B Cells. *J. Immunol.* **163,** 1321 LP-1326 (1999).

88. Ricci, F. *et al.* Patient-derived ovarian cancer xenografts re-growing after a cisplatinum treatment are less responsive to a second drug re-challenge: a new experimental setting to study response to therapy. *Oncotarget* **8,** 7441–7451 (2017).

89. Wang, L. *et al.* Chromatin accessibility regulates chemotherapy-induced dormancy and reactivation. *Molecular therapy. Nucleic acids* **26,** 269–279 (2021).

90. Saitoh, M. Involvement of partial EMT in cancer progression. *J. Biochem.* **164,** 257–264

(2018).

91. Nevo, J. Novel Players in the Integrin Signaling Orchestra: TCPTP and MDGI. (2021).

7.PUBLICATIONS

"Splicing factor proline- and glutamine-rich (SFPQ) protein regulates platinum response in ovarian cancer-modulating SRSF2 activity". Ilenia Pellarin, Alessandra Dall'Acqua, Alice Gambelli, Ilenia Pellizzari, Sara D'Andrea, Maura Sonego, Ilaria Lorenzon, Monica Schiappacassi, Barbara Belletti & Gustavo Baldassarre, Oncogene. https://doi.org/10.1038/s41388-020-1292-6.

"Cutaneous adverse reactions after m-RNA COVID-19 vaccine: early reports from Northeast Italy". Farinazzo E, Ponis G, Zelin E, Errichetti E, Stinco G, Pinzani C, Gambelli A, De Manzini N, Toffoli L, Moret A, Agozzino M, Conforti C, Di Meo N, Schincariol P, Zalaudek I. J Eur Acad Dermatol Venereol. 2021 May 22:10.1111/jdv.17343. doi: 10.1111/jdv.17343. Epub ahead of print. PMID: 34021625; PMCID: PMC8242497.

8.ACKNOWLEGMENTS

This PhD project was conducted in Division of Molecular Oncology, Centro di Riferimento Oncologico di Aviano (CRO) IRCCS, National Cancer Institute.

I want to thank all my lab group members for being such a great part of my life these years. In particular Dr. Gustavo Baldassarre for accepting me in the lab and giving me the opportunities to carry out my PhD project and to Dr. Maura Sonego for teaching me and giving all the supports I needed over the years.